Earth and Planetary Science Letters, 90 (1988) 273–296
Elsevier Science Publishers B.V., Amsterdam – Printed in The Netherlands

[1]

Heterogeneous mantle domains: signatures, genesis and mixing chronologies

Stanley R. Hart

Department of Earth, Atmospheric and Planetary Sciences, Massachusetts Institute of Technology, 77 Massachusetts Avenue, Cambridge, MA 02139 (U.S.A.)

Received January 6, 1988; revised version accepted May 31, 1988

A Sr-Nd-Pb isotope data base is available now which includes over 300 samples from some 43 oceanic islands or island groups. This data base supports the identification by Zindler and Hart [20] of four principal end-member isotopic components in oceanic basalts: depleted MORB mantle (DMM), high U/Pb mantle (HIMU) and two enriched mantle components (EMI, EMII). Linear mixing arrays (in five isotopic dimensions) between EMI and HIMU and between DMM and HIMU are documented and argue for similar proportions of Sr-Nd-Pb in these three components. EMI is argued to be a slightly modified bulk-earth component; HIMU is a component with a greatly enhanced U/Rb ratio, probably generated by intra-mantle metasomatism. It is unlikely that either EMI or HIMU are recycled oceanic crust or sediment. EMII is easily reconciled with a recycled (subducted) sediment protolith; this leads to strong Pb enrichment and consequently to markedly curved mixing arrays between EMII and the other components.

The DUPAL anomaly is demonstrated to be unequivocally real, and is marked by basalts with enhanced contents of EMI, EMII, or HIMU; polar regions are marked by only weak or absent signatures from these components. Not all basalts from the DUPAL belt show a strong DUPAL signature, but 95% of all basalts showing a strong DUPAL signature lie between 0° and 50° south latitude.

The mesosphere boundary layer model of Allègre and Turcotte [21] is shown to be consistent with available data, provided a somewhat ad-hoc plea is made for preferential recycling of sediments and delaminated continental lithosphere within the DUPAL latitudes. An alternative model is proposed which links the DUPAL with other deep mantle geophysical anomalies, and utilizes a core/mantle boundary layer as a source of the DUPAL components. The low-degree mantle circulation is viewed as whole mantle quadrupolar convection, with equatorial upwelling; this serves to concentrate DUPAL components (and hotspots themselves) into the low-latitude regions.

1. Introduction

We are approaching the silver anniversary of the first evidence for isotopic heterogeneities in the earth's mantle [1–3]. We have learned a great deal in these 25 years: the heterogeneities exist on both small scales [4,5] and very large scales [6,7]; substantial correlations exist between various isotopic tracers [8–11,102–105]; the age of development of the heterogeneities is of the order of several billion years [12–14], and there is a first-order isotopic distinction between the mantle which supplies ocean ridges and that which supplies oceanic islands [15,16]. These findings have gained widespread acceptance as major constraints on models of mantle evolution and dynamics [17–19,21,66]. And yet, with our present arsenal of some 9 or 10 different isotopic tracers, and mass spectrometers which are building a very formidable data base with a speed and precision undreamed of 25 years ago, we still lack answers to numerous first-order questions. How many discrete mantle domains exist, where are they located, and how do they form? Are heterogeneities being created faster than they are being convectively destroyed? Do primitive undifferentiated reservoirs still exist on earth? In subsequent sections, I will review the existing Sr, Nd and Pb isotopic data relevant to oceanic mantle domains, and will show how some new and novel considerations of these isotopic tracer data can further our understanding of these unsolved questions. The rare gas isotopes are also relevant to this discussion, but I have not attempted to include them here.

2. Methodology and approach

Except for a specific discussion of continental basalts in section 8, the data set and plots used

0012-821X/88/$03.50

here are restricted to volcanic rocks from oceanic regions (the only exception being two samples from Nunivak Island on the Alaskan Continental shelf). For the most part, data are limited to samples of Cenozoic age (exceptions here being Walvis Ridge, Rio Grande Rise and the New England Seamounts, where ages of up to 100 Ma are involved). Samples are largely restricted to basaltic eruptive rocks (a few tracybasalts are included, as are a few gabbros; no trachytes or more differentiated rocks are included). Only data involving determination of Sr, Nd and Pb on the same sample are used (see Fig. 13 caption for one exception). In so far as possible, the Pb data are normalized to absolute ratios through NBS standards, and the Sr and Nd data are adjusted to 0.70800 for the E&A standard and 0.51264 for the BCR-1 standard, respectively.

The total data base compiled for use here consists of 318 samples from 43 islands or island groups. No MORB are included in this data base, though MORB fields or an average MORB point may be plotted in some of the figures for reference. Not all of the available Hawaiian data are used; individual sample data for Koolau, Lanai, and Kahoolawe are used, otherwise only the averages for Loihi, Kilauea, Mauna Loa, Haleakala, Honolulu series, Waianae and La Perouse Pinnacles are used. I will not attempt to list all of the localities and data references involved in this data set; many of the publication references may be found in [7,22]. New data published subsequently may be found in [23–50].

3. Identification of components

The oceanic data set discussed above is plotted on conventional Sr-Nd-Pb isotope correlation diagrams (Figs. 1, 2 and 3). Following Zindler and Hart [20], I will choose the least number of end-member "components" with which the data may be circumscribed. Furthermore, these components will be located close to the various extremes of the data arrays; this is partly a matter of convenience, and partly constrained by the data itself. As a heuristic matter, the components are deemed to be homogeneous and of fixed isotopic composition; clearly, there may be significant heterogeneity involved, but as long as this heterogeneity is small compared to the range of data overall, subsequent arguments will not be invalidated.

Zindler and Hart [20] concluded that four components were adequate to circumscribe the data and termed these DMM (depleted MORB mantle),

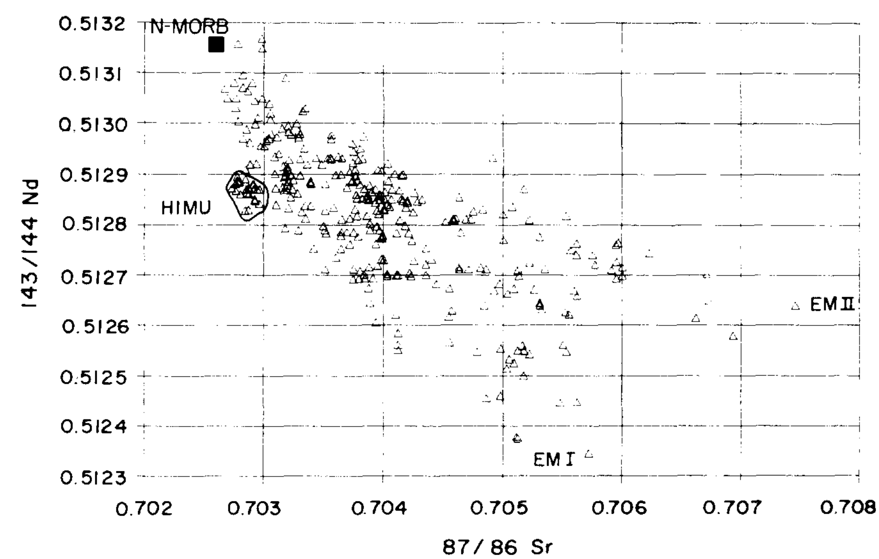

Fig. 1. Nd-Sr isotope correlation plot for 318 oceanic island basalts (OIB). Three putative mantle components HIMU, EMI and EMII are approximately indicated; a field is drawn around HIMU samples from St. Helena, Tubuaii and Mangaia. The filled square is the average of 125 N-type MORB from White et al. [31]; the location of DMM is not shown, but would lie near or to the northwest of the N-MORB point. Data references given in text.

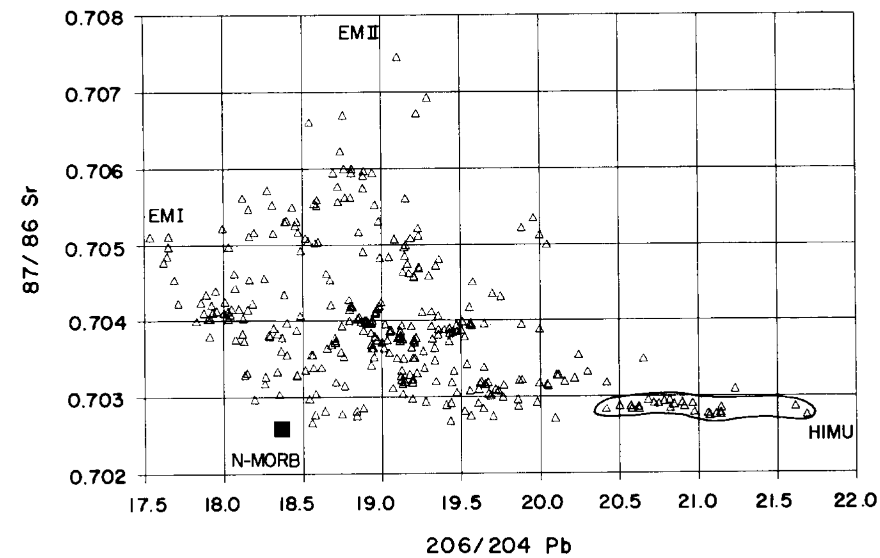

Fig. 2. Sr-Pb isotope correlation plot for 318 OIB. See Fig. 1 legend for details.

HIMU (high U/Pb) and two enriched mantle components (EMI and EMII); this specification of components appears necessary and sufficient. The fifth possible component defined by Zindler and Hart [20] (PREMA, for prevalent mantle) may exist but is not clearly required by the data. The justification for these components can be seen by studying Figs. 1–3. HIMU is characterized by high $^{206}Pb/^{204}Pb$ and low $^{87}Sr/^{86}Sr$ and is most clearly seen in Figs. 2 and 3. DMM is not plotted as such, but an average "normal MORB" (N-MORB) is shown by the filled square (this is the average of 125 Atlantic and Pacific N-MORB as tabulated by White et al. [31]). DMM would presumably lie to more extreme isotopic ratios, as perhaps exemplified by the highest or lowest values measured in any N-MORB (0.7022, 0.5133 and 17.3, for example). The enriched components are so designated because they have Sr and Nd isotopic ratios demonstrating a growth history in reservoirs of high (enriched) Rb/Sr and Nd/Sm. While the need for an "enriched" component has long been recognized [51], it is now clear that two quite distinct EM components are required [20]. EMI has very unradiogenic $^{206}Pb/^{204}Pb$ (rivaled only by a few MORB samples), and the lowest $^{143}Nd/^{144}Nd$ present in the oceans. EMII has the highest $^{87}Sr/^{86}Sr$ of all oceanic mantle, coupled with intermediate $^{206}Pb/^{204}Pb$ and $^{143}Nd/^{144}Nd$.

With regard to the "uniformity" of these components, it is interesting to note that the dispersion of data decreases substantially as HIMU is approached, and that for samples with $^{206}Pb/^{204}Pb$ greater than 20.5, only rather restricted ranges of Sr, Nd and $^{208}Pb/^{206}Pb$ exist. This suggests that HIMU, at least, is a rather uniform component. Assessment of the uniformity of EMI is difficult at this point, as there is only one locality (Walvis Ridge) where this component shows up as an extremum. EMII is present as a dominant component in Samoa, the Society and Marquesas Islands and Kerguelen, and appears to be possibly the least uniform of the four components, showing significant dispersion in $^{206}Pb/^{204}Pb$ or $^{143}Nd/^{144}Nd$ at a given $^{87}Sr/^{86}Sr$.

Other authors have argued for either additional components, or different "placement" of the ones enumerated above. White [52] proposed five oceanic mantle reservoirs, based on five "groupings" of oceanic basalts, as opposed to the end-member component approach used here. Four of White's groups may be "affiliated" with components used here (MORB = DMM, Society = EMII and St. Helena = HIMU, Hawaii = EMI); I would suggest his Kerguelen group is a mixture of EMI and EMII. Zindler et al. [22] identified an enriched component with the Tristan-Gough-Kerguelen (TGK) data groupings; I would also suggest that

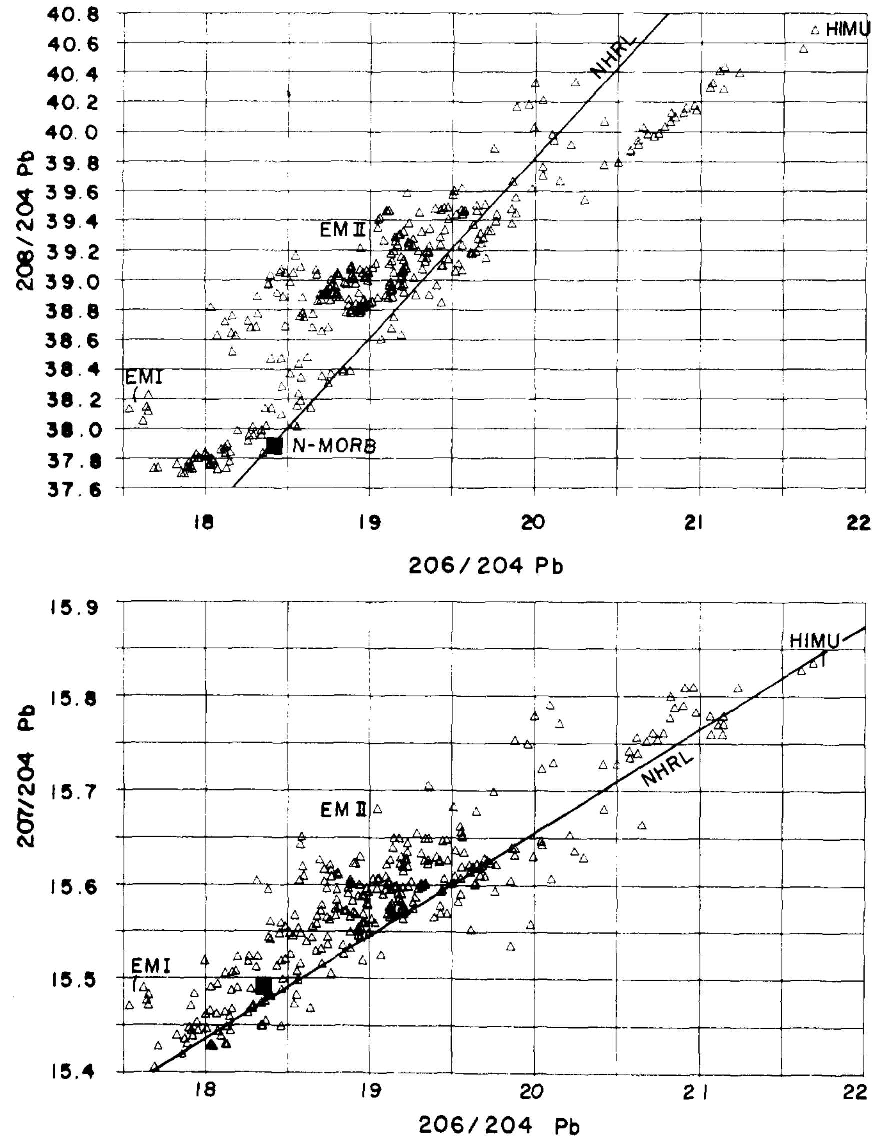

Fig. 3. Pb-Pb isotope correlation plot for 318 OIB. The northern hemisphere reference line (NHRL) of Hart [7] is shown; other details as in Fig. 1. Much of the Pb data used to define the NHRL are not shown in this Figure, as they do not have accompanying Sr and Nd data; this explains why the NHRL does not seem to be "aligned" with any particular concentration of data points.

these data are better considered as mixtures of EMI and EMII. Allègre and Turcotte [21] also designated a TGK component; they did not recognize an EMI component because they did not consider the Walvis data set of Richardson et al. [51]. Allègre and Turcotte also designated a second EM component, São Miguel, which is higher in $^{206}Pb/^{204}Pb$ and $^{143}Nd/^{144}Nd$ than their TGK component. This was further emphasized through principal component analysis by Allègre et al. [53].

It would appear (C.J. Allègre, personal communication; [36]) that the São Miguel component may instead be a mixture of EMII and HIMU, though this would require either or both of these components to have higher $^{207}Pb/^{204}Pb$ and $^{208}Pb/^{204}Pb$ than envisioned in Fig. 3 (the São Miguel data, at $^{206}Pb/^{204}Pb \sim 20$, lies above a line joining EMII and HIMU). In any event, the São Miguel component is closely allied with the EMII component as defined here.

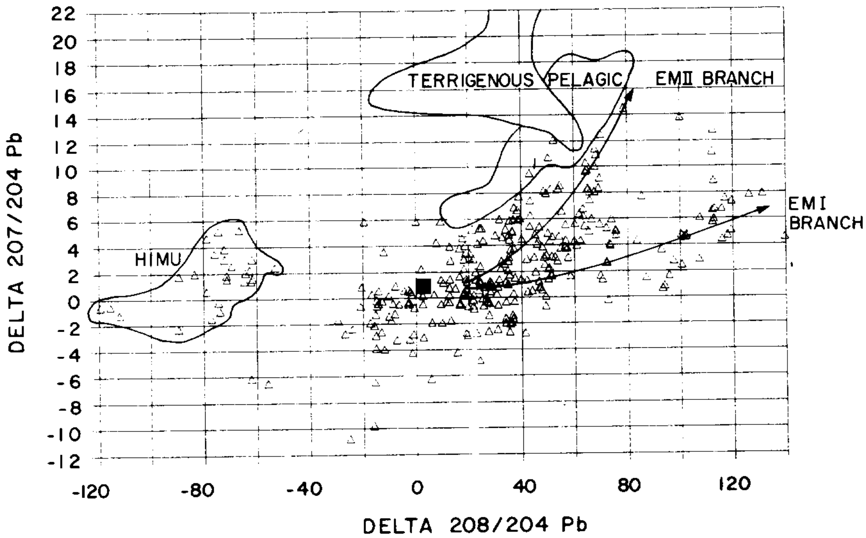

Fig. 4. ΔPb correlation plot for 318 OIB. $\Delta^{207}Pb/^{204}Pb$ and $\Delta^{208}Pb/^{204}Pb$ are the vertical deviations in $^{207}Pb/^{204}Pb$ and $^{208}Pb/^{204}Pb$ from the northern hemisphere reference line (NHRL) of Hart [7]. The filled square is N-MORB; see Fig. 1 caption for other details. The field marked "terrigenous" encloses the western Atlantic terrigenous sediments of White et al. [79]; the field marked "pelagic" encloses 52 analyses of clay-rich pelagic sediment (data from Barreiro [90]; Church [91]; Reynolds and Dasch [92]; Sun [10]; Vidal and Clauer [93]). The use of this plot for elucidating sediment contamination in arc lavas has been discussed by Salters et al. [94].

The only isotopic relationships which are not well depicted in Figs. 1–3 are those between $^{207}Pb/^{204}Pb$ or $^{208}Pb/^{204}Pb$ and Sr or Nd. Hart [7] defined a northern hemisphere reference line (NHRL) for Pb, with vertical deviations from this line being termed either Δ7/4 Pb or Δ8/4 Pb; he also showed a general positive correlation (in OIB) between these ΔPb parameters and between them and $^{87}Sr/^{86}Sr$. Figs. 4 and 5 show these relationships; Fig. 4 shows a general positive correlation between Δ7/4 Pb and Δ8/4 Pb, but with two "branches"—one curving up toward EMII and one flatter branch directed toward EMI. This contrasting behaviour of the two EM trends will be

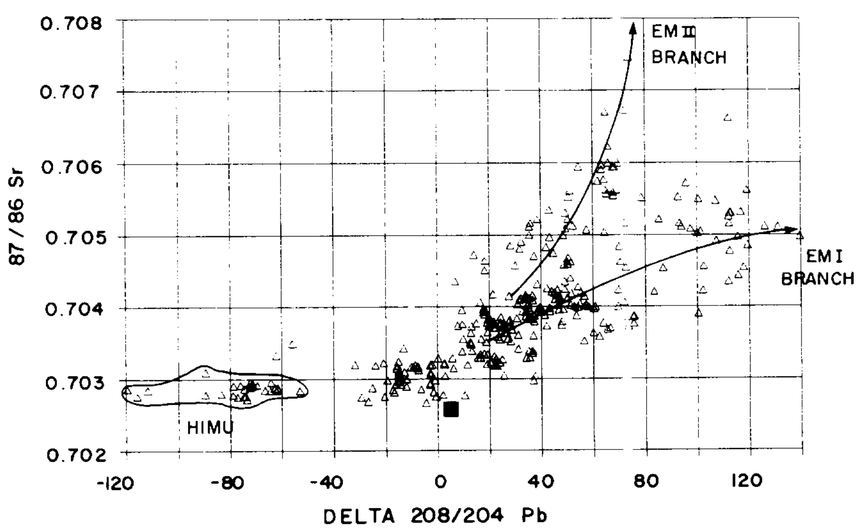

Fig. 5. $^{87}Sr/^{86}Sr-\Delta^{208}Pb/^{204}Pb$ correlation plot for 318 OIB; details as in Fig. 4 caption.

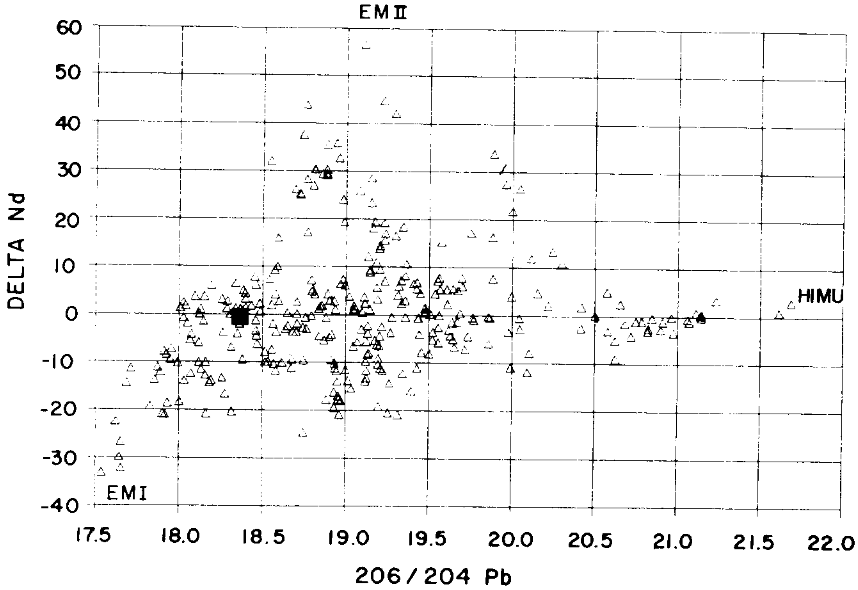

Fig. 6. ΔNd versus $^{206}Pb/^{204}Pb$ correlation plot for 318 OIB. Filled square is average N-MORB. ΔNd is vertical deviation from mantle plane of Zindler et al. [22], as discussed in Hart et al. [54]. A ΔNd of 10 units corresponds to 2 ϵ_{Nd} units. The horizontal line at ΔNd = 0 is the projection of the mantle plane.

utilized below in discussing the genesis of the EM components. Note also the clear dislocation of the HIMU data group to the left on this plot (the HIMU islands fall on the NHRL for $^{207}Pb/^{204}Pb$ but fall well below it for $^{208}Pb/^{204}Pb$—Fig. 3). Fig. 5 shows that there is also a general positive correlation between $^{87}Sr/^{86}Sr$ and Δ8/4 Pb, again with two EM branches.

Hart et al. [54] showed that a particularly useful plot for discriminating between the EMI and

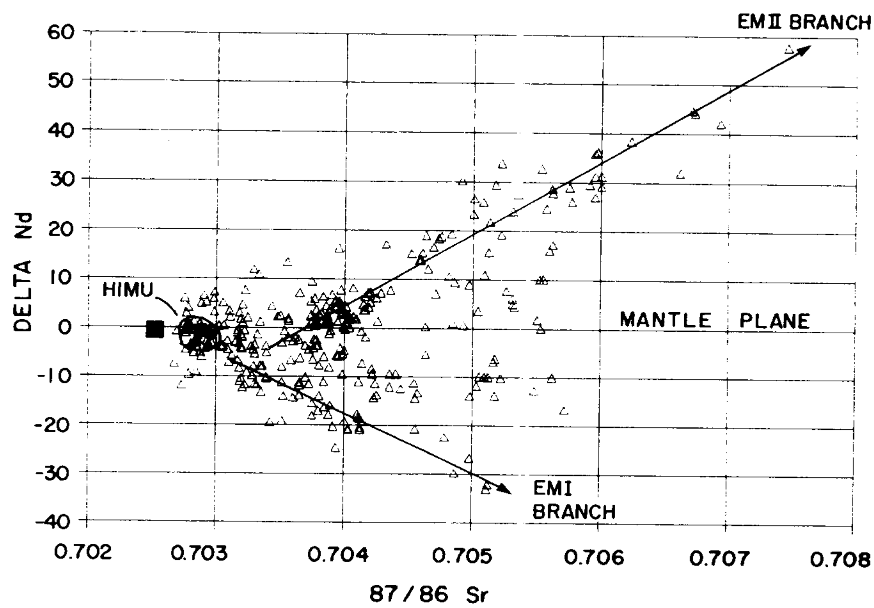

Fig. 7. $\Delta Nd-^{87}Sr/^{86}Sr$ correlation plot for 318 OIB; details as in Fig. 1 and Fig. 6 captions.

EMII components was one employing the vertical deviation in $^{143}Nd/^{144}Nd$ from the mantle plane of Zindler et al. [22] used as a reference surface. Positive values of ΔNd signify samples lying *above* the mantle plane, whereas negative values of ΔNd signify samples lying *below* the mantle plane. The mantle plane thus appears as a horizontal reference line in Figs. 6 and 7. EMI has strongly negative ΔNd and EMII has strongly positive ΔNd (DMM and HIMU lie on the plane by definition). Fig. 8 shows that ΔNd and $\Delta 8/4$ Pb (or $\Delta 7/4$ Pb, not shown) are also correlated; in this case, the EMI branch has a negative slope and the EMII branch has a positive slope. As a point of interest, Figs. 6–8 show that a significant fraction of all oceanic basalts fall off the mantle plane. If we take ± 4 units in ΔNd as a typical analytical precision [54], and ± 8 units as a reasonable limit to encompass various interlaboratory biases and geologic noise (alteration, etc.), then in fact, *41%* of the 318 samples in the data base are significantly "off" the mantle plane. However, since only two components now lie in the mantle plane, the fact that 59% of the data lie close to the plane is only an expression of the fact that DMM and/or HIMU are significant components in many oceanic basalts. While I have not done the fitting, it would appear from Figs. 6 and 7 that a plane (or mantle "plate" of Allègre et al. [53]) passing through either DMM–HIMU–EMII or DMM–HIMU–EMI would contain a larger fraction of all available data. In any event, the oceanic data are not describable as a plane or plate, but rather as a narrow plate (between DMM and HIMU) with two conical appendages tapering out toward EMI and EMII.

4. The island-component connection

First, for convenience, the four components elucidated above are identified with certain isotopically extreme samples (see Figs. 9, 10 and 11). The actual isotopic character of the components may in fact be more extreme than any measured samples, but this will be difficult to confirm unless sample mixing arrays are found which converge on a component from two intersecting directions. I will argue below that there is both an EMI–HIMU array and a DMM–HIMU array, and the intersection of these two arrays is approximately at a $^{206}Pb/^{204}Pb$ ratio of 21–21.5, which is the observed value for Tubuaii and Mangaia. In other words, HIMU is probably not located at a $^{206}Pb/^{204}Pb$ of 25, with no currently observed data being a "pure" HIMU; Mangaia is close to pure HIMU. The "purest" HIMU thus

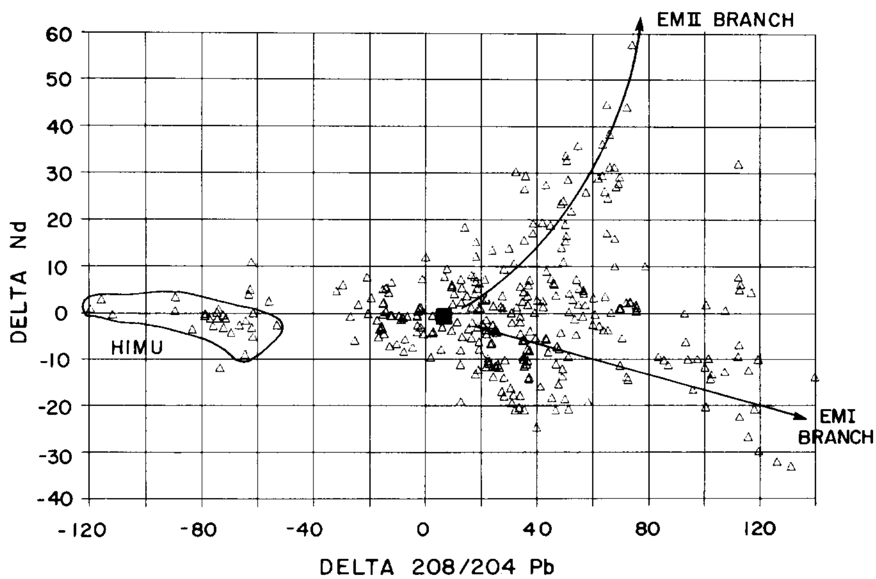

Fig. 8. ΔNd–$\Delta^{208}Pb/^{206}Pb$ correlation plot for 318 OIB. Axes as defined in captions to Fig. 4 and Fig. 6; other details as in Fig. 1 caption.

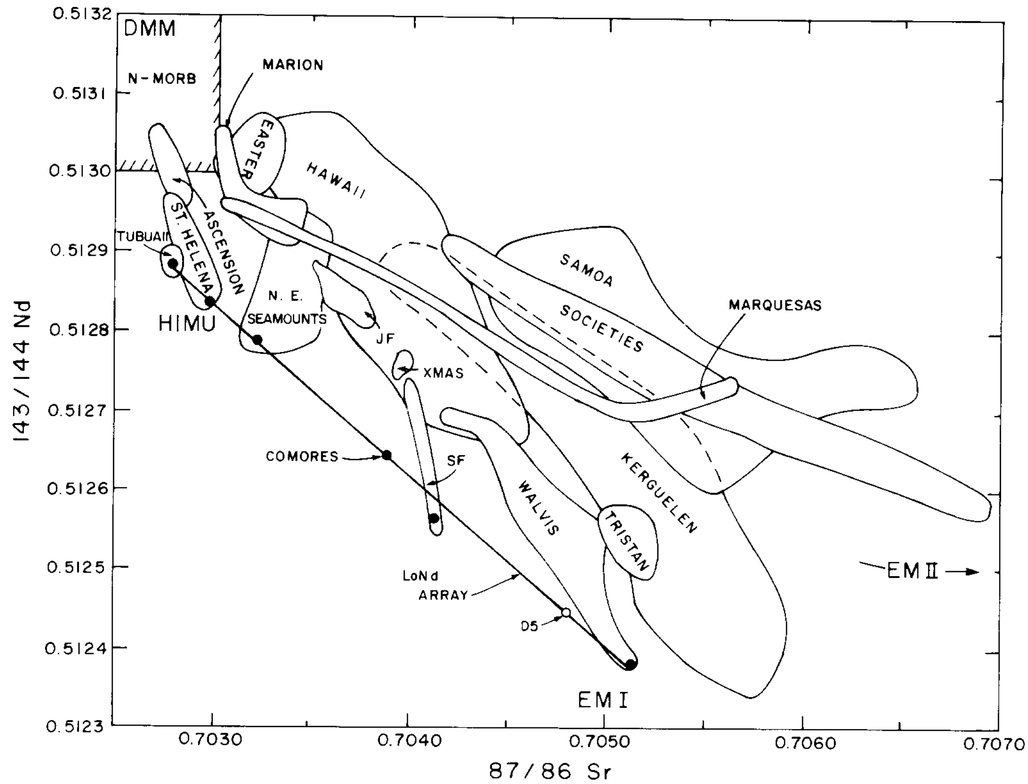

Fig. 9. Nd-Sr isotope correlation plot showing fields for selected oceanic islands. The line marked "NoNd array" connects the lowest Nd samples from each of the indicated fields; this line is linear in five-dimensional isotopic space [54]. Also shown is the peculiar Indian Ocean dredge sample D5 from Hamelin and Allègre [56].

occurs at St. Helena (central Atlantic) and at Mangaia, Rurutu, Tubuaii and Rimatara (Cook-Austral Islands, southwest Pacific [28,55]).

EMI is defined by the near-crest samples from the Walvis Ridge [51] and there are no other known basalts that are relatively "pure" EMI. A sea-floor basalt dredged from the Southwest Indian Ridge (D5 of Hamelin and Allègre [56]) is EMI in character, with even lower $^{206}Pb/^{204}Pb$ than Walvis, but with less extreme values of Sr and Nd. Koolau volcano (Oahu) shows a mixing array which is clearly headed toward EMI as one end-member, but the most extreme sample (69TAN-2, Table 1) still has a $^{143}Nd/^{144}Nd$ of 0.51265, as opposed to the extreme Walvis values of 0.51238. Because of the lack of data arrays in and around EMI, it is particularly difficult to say whether EMI should be placed at the end of the Walvis array or at a much more extreme location; the Koolau array suggests the $^{206}Pb/^{204}Pb$ of EMI is not lower than 17.5, but this is not strongly constrained.

The most distinguishing characteristic of EMII is the high $^{87}Sr/^{86}Sr$ value; of the four highest values in the present data set (0.7067–0.7074), three are from Samoa [29] and one is from Tahaa, Society Islands [52,57]. Basalts from the Marquesas [33,41,58] clearly define an array which is headed toward EMII, however, the highest Sr value is only 0.7056 (see Fig. 10). As with EMI, it is difficult to know whether the most extreme available sample (0.7074) is more or less pure EMII, or whether EMII lies at a more extreme $^{87}Sr/^{86}Sr$ value than any yet observed.

For MORB, there is a great deal of data available and it seems unlikely that significantly more extreme samples are going to be found. The lowest $^{206}Pb/^{204}Pb$ values are typically found in the Indian Ocean (lowest value is 17.3 for N-MORB); however, the lowest Sr and highest Nd ratios are

TABLE 1

SR, Nd and Pb isotopic data, oceanic basalts

Island/ Sample No.	$^{87}Sr/^{86}Sr$	$^{143}Nd/^{144}Nd$	$^{206}Pb/^{204}Pb$	$^{207}Pb/^{204}Pb$	$^{208}Pb/^{204}Pb$
Balleny (Sabrina)					
24583	0.70297	0.51296	19.856	15.605	39.482
24591	0.70300	0.51296	19.762	15.594	39.399
Christmas					
XI-1	0.70399	0.51278	18.869	15.597	38.835
XI-2	0.70394	0.51276	19.123	15.627	39.180
XI-3	0.70399	0.51278	18.900	15.623	39.017
XI-4	0.70397	0.51279	18.914	15.623	38.979
XI-5	0.70399	0.51278	18.869	15.591	38.871
Koolau (Oahu) [a]					
WW9991	0.70380	0.51286	17.909	15.471	37.758
69Tan-2	0.70455	0.51265	17.686	15.406	37.735
Indian Ocean Crust (DSDP)					
250A-26-6 *	0.70299	0.51294	19.580	15.624	39.325
254-31-1 *	0.70431	0.51278	18.042	15.508	38.536
256-11-1 *	0.70424 **	0.51281	19.432	15.605	39.397
Marion / Prince Edward					
WJE 21	0.70305	0.51302	18.574	15.541	38.302
WJM 39	0.70336	0.51292	18.506	15.541	38.329
WJM 43	0.70339	0.51288	18.560	15.546	38.395
AJE 1M	0.70339	0.51290	18.608	15.532	38.440
Nunivak [b]					
B-5	0.70298	0.51315	18.539	15.473	38.031
B-10	0.70282	0.51307	18.637	15.469	38.144
La Perouse Pinnacle					
LPPE-15 *	0.70352	0.51296	18.554	15.489	38.188
LPPW-20 *	0.70364	0.51294	18.557	15.493	38.197
LPPW-30 *	0.70354	0.51295	18.580	15.495	38.206
Ponape					
1	0.70329	0.51297	18.462	15.489	38.289
2	0.70327	0.51295	18.448	15.483	38.263
4	0.70335	0.51296	18.573	15.516	38.366
Rio Grande Rise					
516F-128-2 (plag)	0.70478	0.51255	17.619	15.490	38.054

Analytical techniques as described in Taras and Hart [49].

* HCl-leached powders

** Sr done on plagioclase separate

[a] Sr and Nd data from Roden et al. [101].

[b] Sr and Nd data from Roden [87].

Sr and Nd reported relative to 0.70800 for E&A, and 0.512620 for BCR-1. Pb corrected, ratio by ratio, using SRM 981 and values of Todt et al. [89].

not found on these extreme Pb samples but rather on MORB from the Mid-Atlantic Ridge. I suspect the low $^{206}Pb/^{204}Pb$ values of Indian Ocean MORB are not representative of the pure DMM reservoir, but rather represent mixing of a DMM with $^{206}Pb/^{204}Pb$ in the 17.8–18.2 range with either an EMI component, or the EMI-like material exemplified by D5 (there is a clear tend-

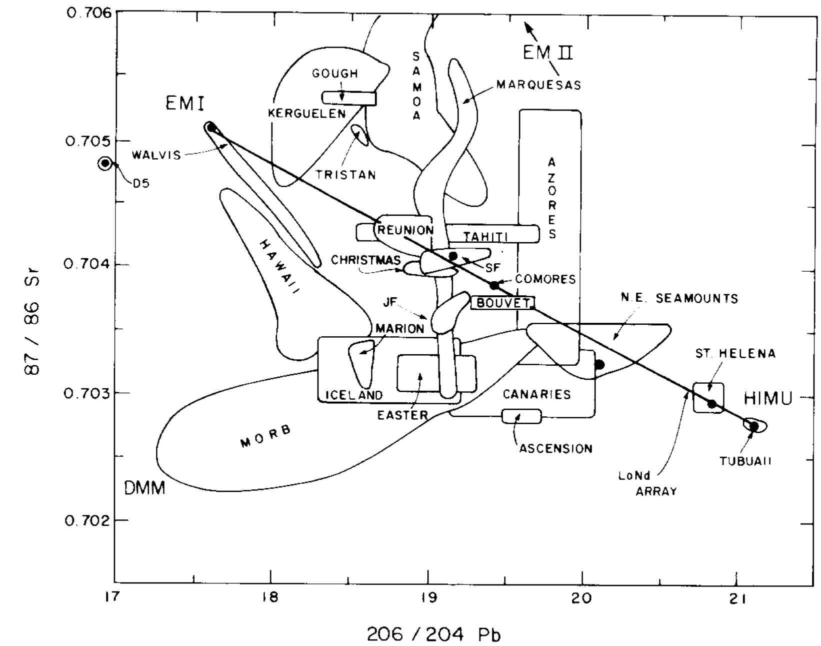

Fig. 10. Sr-Pb isotope correlation plot showing fields for selected oceanic islands. Further details are given in Fig. 9 caption.

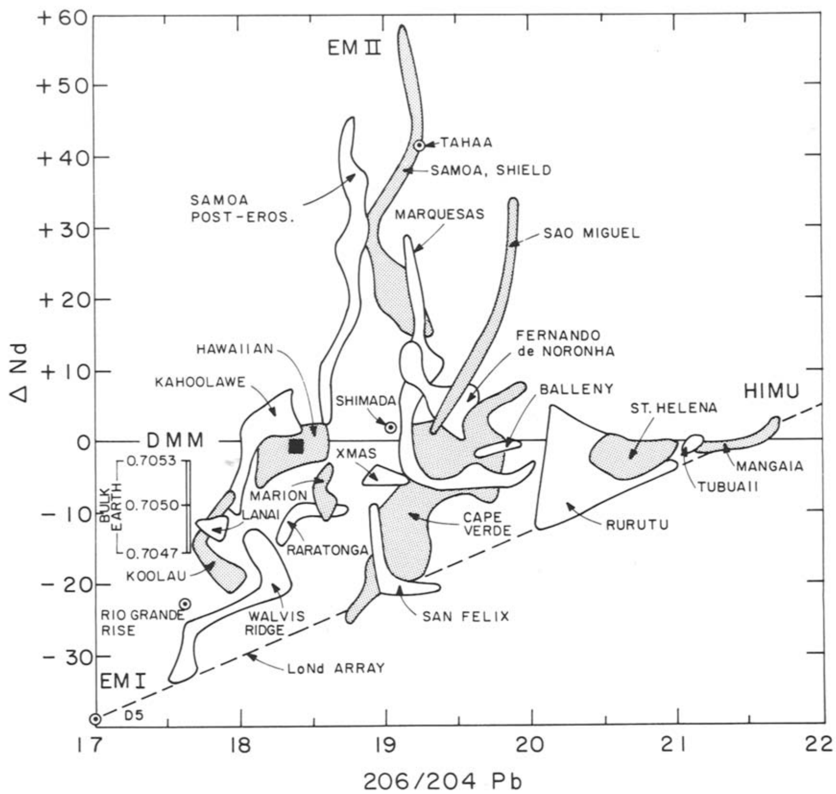

Fig. 11. $\Delta Nd-{}^{206}Pb/{}^{204}Pb$ isotope correlation plot showing fields for selected oceanic islands. The field marked "Hawaiian" encloses averaged data points for Loihi, Kilauea, Mauna Loa, Haleakala (four series), Honolulu series, Waianae and La Perouse Pinnacles. The LoNd array of Hart et al. [54] is shown by the dashed line. The locus of possible bulk-earth compositions is shown by the vertical bar on the left side; a geochron Pb of 17.62 (single stage = 8.1) was chosen, and bulk-earth Nd assumed to be chondritic (= 0.512638). Various bulk earth Sr values ranging from 0.7047 to 0.7053 are indicated; for bulk earth to lie on the mantle plane would required a Sr isotope ratio of 0.7054.

ency for the MORB samples with the lowest $^{206}Pb/^{204}Pb$ values to also have negative ΔNd values and high $\Delta 8/4$ Pb).

5. Global distribution of components

The global distribution of these four isotopic components is far from random, as shown in Figs. 12 and 13. The two EM components are characterized by high $^{87}Sr/^{86}Sr$ and high $\Delta 8/4$ Pb, with EMII best mapped with $^{87}Sr/^{86}Sr$, and EMI best mapped with $\Delta 8/4$ Pb. With few exceptions, both EM components are restricted to the southern hemisphere in a belt between the equator and 50°S. These EM components were the ones used to define the DUPAL anomaly [7], though at that time the two EM components were lumped together. Depending on exactly what criteria are used to define the "presence" of EMI or EMII (in Figs. 12 and 13, I define $^{87}Sr/^{86}Sr > 0.705$ and $\Delta 8/4$ Pb $> +60$ as "DUPAL"), the only exceptions to the restriction of these EM components to the southern hemisphere is the EMII (high $^{87}Sr/^{86}Sr$) signature at São Miguel (39°N latitude, Fig. 12) and the EMI ($\Delta 8/4$ Pb) signature at Koolau, Oahu (21°N latitude, Fig. 13) and at Shimada Seamount (17°N latitude, Fig. 13 [23]). The notion of a DUPAL anomaly has been criticized both because DUPAL samples have been found in the northern hemisphere, and because many samples from within the DUPAL belt do not show the EM signature. Clearly the fact that only 3 out of 55 samples with $^{87}Sr/^{86}Sr > 0.7050$ (or 5 out of 82 samples with $^{87}Sr/^{86}Sr > 0.7045$) or 3 out of 70 samples with $\Delta 8/4$ Pb $> +60$, lie in the northern hemisphere is fairly impressive evidence that EMI and EMII are southern hemisphere components. Originally, I defined the DUPAL [7] on the basis of isotopic data *averaged by island*; as is evident from Figs. 9–11, most islands, and particularly those with marked EM signatures, show large intra-island isotopic variations with the EM (DUPAL) components being diluted in many samples with DMM or HIMU. Obviously, an island may have a strong DUPAL signature "on average", without every sample showing a DUPAL signature. While the "clarity" with which the DUPAL belt may be mapped depends on the comprehensiveness of the data sets for particular islands, there can be no doubt that

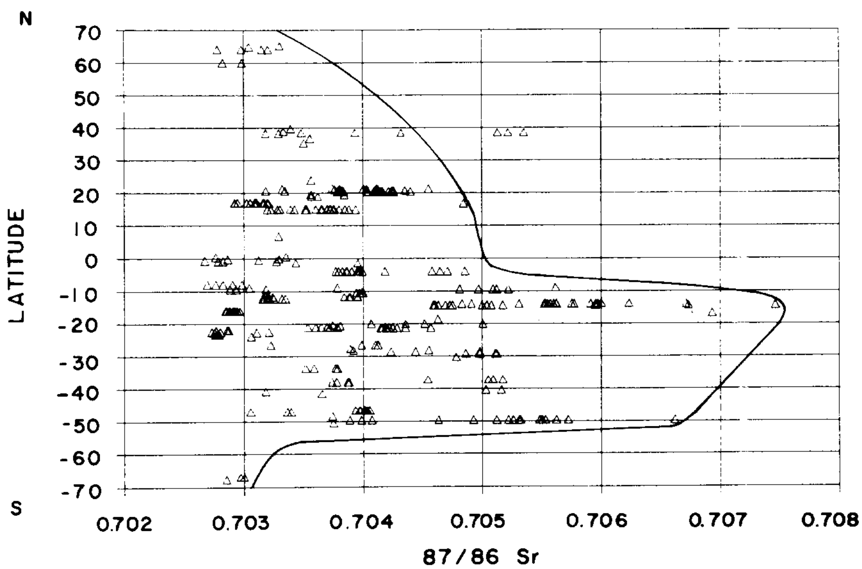

Fig. 12. $^{87}Sr/^{86}Sr$ ratio versus sample latitude plot for 318 OIB. The DUPAL signature is here delineated as values > 0.705, but the curve is drawn to emphasize possible pole-ward gradients as well. As drawn, only São Miguel (Azores) has a DUPAL signature that lies outside the DUPAL belt. If DUPAL signature is instead taken to be Sr ratios > 0.704, then Shimada Seamount and Koolau, Kahoolawe and Lanai (Hawaii) would also fall outside the DUPAL belt. A great deal of additional Sr isotope data exist in the literature (unaccompanied by Nd and Pb data) which would serve to fill in much of the area to the left of the curve, without transgressing the curve.

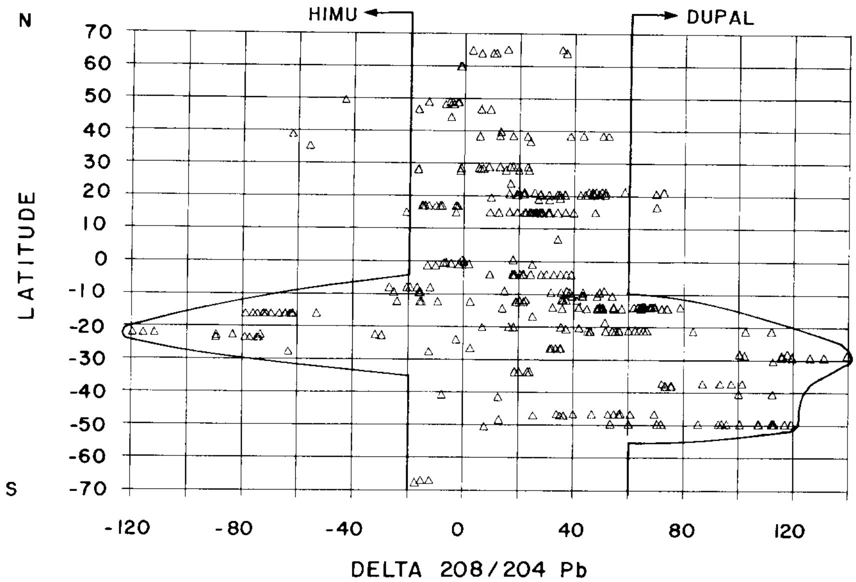

Fig. 13. $\Delta^{208}Pb/^{204}Pb$ versus sample latitude plot for 348 OIB. In this case, the data set has been augmented with "Pb only" data from the Canaries and Guadalupe [10] and the northeast Pacific Seamounts [59]. The DUPAL is delineated here as samples with $\Delta 8/4$ Pb > +60; only three samples outside the DUPAL belt have $\Delta 8/4$ Pb > +60 (one sample each from Koolau, Lanai and Shimada Seamount). Note that HIMU islands can be delineated at $\Delta 8/4$ Pb values less than −20; within the DUPAL belt these include Mangaia, Tubuaii, St. Helena, Rimatara, and Rurutu. Only three samples lying outside the DUPAL belt have HIMU-like $\Delta 8/4$ Pb signatures.

the EM components are dominantly situated in the southern hemisphere.

Whether or not the DUPAL belt is "continuous" around the world is another debated issue. While there is no argument that one strong DUPAL domain exists between the Mid-Atlantic Ridge and the central Indian Ocean, and that another exists in the west and central Pacific, the intervening areas are less clear-cut. With the presence of Australia and South America masking part of the belt, and a lack of islands in other key areas (eastern Indian Ocean, western Atlantic Ocean), it may never be possible to answer this particular question. Nevertheless, with the data base increased by some 50% since the DUPAL paper was written, the contouring of the maps [7, fig. 2] needs very little alteration; the DUPAL anomaly may be visualized as a ridge-like circum global belt with several prominent peaks on it.

The essential restriction of the HIMU component to the southern hemisphere is also clearly shown in Fig. 13; the only samples with $\Delta 8/4$ Pb values < 25 which lie in the northern hemisphere are two from the New England Seamount chain [49] and one from Union Seamount (northeast Pacific) [59]. While this restriction of HIMU to the southern hemisphere was noted by Hart [7] and Allègre et al. [60], its apparent "connection" with the DUPAL belt has been more forcefully noted by Staudigel et al. [61]. Almost pure HIMU and EMI appear juxtaposed in the Atlantic (St. Helena to Walvis Ridge, ~ 1700 km), while pure HIMU and intermediate EM components are very closely juxtaposed in the western Pacific (Mangaia to Mauke or Raratonga, ~ 200 km [28,55]). It should be emphasized, however, that HIMU is not a ubiquitous feature of the DUPAL belt; whereas there are many DUPAL hotspots erupting EM components, there are arguably only two hotspots erupting "concentrated" HIMU (based on the probability that the Cook-Austral HIMU Islands of Mangaia, Rimatara, Rurutu, Tubuaii and Raivavae are expressions of a single hotspot). Hart at al. [54], in discussing the LoNd array (see Figs. 9 and 10), argued that this array was produced by mixing of HIMU and EMI, and that these two components were therefore spatially, if not genetically, related. There is no obvious HIMU–EMII counterpart to the LoNd array (a HiNd array), so the meaning of the DUPAL association of HIMU and EMII needs further elucidation.

One intriguing feature of Figs. 12 and 13 is not only the sub-equatorial (DUPAL) concentration of high EM hotspots, but the seeming lack of any EM signature whatsoever in hotspots from polar regions. This was hinted at in the DUPAL paper [7], and since that time several additional polar localities have been studied (Scott and Balleny Islands, close to the Antarctic circle, and Nunivak Island, 60° N; see Table 1). The samples from Scott and Balleny Islands plot close to the mantle plane (Fig. 11) and below the NHRL on Pb-Pb plots; the Nunivak samples, for which Sr and Nd was reported in Roden [87], also plot close to the mantle plane and slightly below the Pb-Pb NHRL. The Scott/Balleny Pb data are very similar to that of Sun [10] from Ross Island, Antarctica, and the low $^{87}Sr/^{86}Sr$ for these localities is also typical of the young basaltic volcanics from Marie Byrd Land, Antarctica [62], which are all $\leqslant 0.7030$. In the North Polar regions, there are to my knowledge no truly oceanic hotspots (not counting Iceland, of course); however, the Nunivak basalts carry mantle xenoliths, so they are likely to be free of continental contamination. The so-called Asian isotopic province of Allègre et al. [60] contains numerous northern localities, but is characterized by relatively high $^{87}Sr/^{86}Sr$ (> 0.704)—the influence of crustal or subcontinental EM components on these basalts is not yet documented. The strong lack of hotspots in polar regions will clearly limit our ability to argue strongly for a polar "anti-DUPAL anomaly," but the evidence thus far suggests a lack of EM components in basalts from polar regions, and perhaps even a systematic equator to North Pole decrease in the EM signature (see data "envelope" in Fig. 12).

6. Mixing arrays

Brief mentioned has already been made of the LoNd array, and the proposition that this results from mixing of EMI and HIMU mantle components. I would like to pursue the question of other mixing arrays between the four designated mantle components, because these hold great potential for understanding the location and evolution of these components. First, to specify some assumptions: I believe most of the large-scale features of isotope arrays are created by mixing of separate mantle reservoirs, not by mixing of melts (i.e., a LOS or SOS model, as described by Zindler et al. [63]). While melt mixing undoubtedly plays a role in creating intra-volcano isotopic variations, I don't believe this is the dominant control for the features delineated in Figs. 9 and 10, etc. Implicit in this assumption is also the notion that the intermediate members of an array represent intermediate mixtures of two end-members components, and are not simply the result of a single-type of process which has operated to a different and variable extent (for example, by variable degrees of metasomatism, or variable degrees of melt extraction). These assumptions are not necessarily defendable as unique; they simply represent my opinion based on the "principle of minimum astonishment".

The LoNd array is shown in Figs. 10 and 11, and was shown by Hart et al [54] to be a linear array in five-dimensional isotopic space. Since that time, no additional data have been reported which lie on this array, so the "existence" of this array is no better substantiated than it was in 1986. In Fig. 11, the Cape Verde field [24] appears to terminate on the LoNd array; this is an artifact of this particular projection, as these low-Nd samples fall to the low-Sr side of LoNd in Fig. 10 (0.7039 at 18.74) and have too low a $^{208}Pb/^{204}Pb$ ratio in plots involving $^{208}Pb/^{204}Pb$.

One other array which is better defined is an array stretching between DMM and HIMU. This is delineated in the following way—if there are four mantle components and we exclude two of them, what is the relationship of the remaining two? Since both DMM and HIMU are defined by low $^{87}Sr/^{86}Sr$ (and the two EM components have high $^{87}Sr/^{86}Sr$), I filtered the OIB data base for samples with $^{87}Sr/^{86}Sr < 0.7030$. The result is shown in Fig. 14. Note that some of the fields contain all the existent data for that particular island (Mangaia, Tubuaii, St. Helena, Balleny, Ascension, Nunivak), whereas others show total fields extending down toward the EM components, and only the low-Sr parts of the fields are shown here (Galapagos, Cape Verde, Marquesas, Rurutu). What is clear in this figure is that a continuum exists between DMM and HIMU, and this array is more or less linear. This same sample

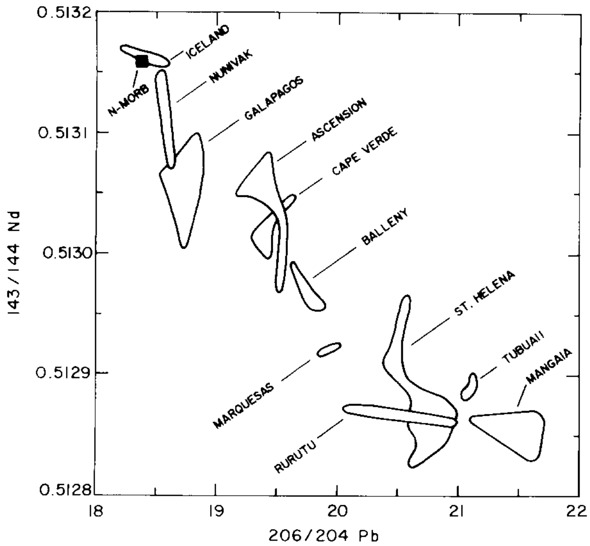

Fig. 14. Nd-Pb isotope correlation plot showing only OIB samples with $^{87}Sr/^{86}Sr < 0.7030$; a total of 52 out of 318 OIB samples passed this criterion, which is essentially a filter against samples containing appreciable EM components.

set is similarly linear on plots of $^{208}Pb/^{204}Pb$ versus $^{206}Pb/^{204}Pb$ or $^{143}Nd/^{144}Nd$, and on Nd-Sr plots—i.e., as with the LoNd array, this array is linear in 5-D isotopic space. I will call this the No-Em array. Also, there is not a marked tendency for island fields to lie *along* the array as a whole, but rather they tend to be oblique or indeterminate in orientation (as is the case with the LoNd array). Note that since DMM and HIMU lie in the mantle plane (by definition), then this array also lies in the mantle plane (its projection is therefore the horizontal line in Fig. 11). As with the LoNd array, it would appear that any given hotspot represented here may be a variable mixture of DMM and HIMU, but a fairly well-mixed mixture. This mixture is then in some cases further mixed with EM components (e.g., Cape Verde, Marquesas) to generate fields stretching toward EM but originating on this No-Em array.

What are the consequences of this observation? They are basically the same as derived from the LoNd array: it would appear that the DMM and HIMU components are located in the mantle in contiguous geometry, such that their mixing can precede mixing with the Em's (just as LoNd is EMI-HIMU mixing followed by mixing to DMM or EMII). Also, because of the approximate linearity in 5-D space, the inference must be that the concentrations of Sr, Nd and Pb, relative to each other, are similar in the DMM and HIMU end-members (as was concluded from the LoNd array for HIMU and EMI). Therefore, for example, Sr/Nd and Pb/Nd concentration ratios must be similar *in all three components* (DMM, HIMU and EMI). What is meant by "similar" is a bit difficult to quantify considering the limited data set which defines LoNd, and the apparent scatter in the case of No-Em. However, simple two-component mixing calculations suggest that the relative concentrations of Sr, Nd and Pb in the DMM and HIMU end members is probably similar to within 30–50%, and certainly within a factor of two. The formal limits on HIMU-EMI are even smaller, but there are really only two data points that define the middle portion of the LoNd array (San Felix and Comores). The statement that, for example, Sr/Pb ratios in DMM, EMI and HIMU are similar to within $\pm 50\%$ may not seem very useful; consideration of the range of materials proposed for EMI and HIMU, however, reveals this limit to be an immensely useful constraint. In the case of EMI, this constraint was used by Hart et al. [54] to rule out recycled pelagic sediment as the protolith for EMI (because of the radically low Sr/Pb ratio of pelagic sediments). Similarly, the proposal [64–66] that HIMU is mantle which has had Pb extracted out of it into the core would lead to high Sr/Pb ratios for HIMU (presuming Sr is not siderophile); this would be inconsistent with the approximate equality established for Sr/Pb between DMM and HIMU by the linearity of the No-Em array.

Note that the intersection of LoNd and No-Em serves to define the isotopic parameters for HIMU. Mangaia is suitable as pure HIMU; a $^{206}Pb/^{204}Pb$ any higher would diminish the linearity of one or the other of these arrays.

Having connected HIMU to both DMM and EMI with mixing arrays, the question then is whether mixing arrays are evident between EMI and DMM, or between EMII and any of the other three components. While there is a series of samples in Fig. 2 which marks a linear "edge" to the data stretching between EMI and N-MORB (these are several Iceland picrites, and the Koolau/Lanai data for Hawaii), there is no obvious array between these components on the Pb-Pb plots (Fig.

3). Thus, I conclude that there is no discernible array between EMI and DMM (or N-MORB).

As for arrays involving EMII, there is nothing obvious between EMII and HIMU (Fig. 3, 6 or 11), EMII and EMI (Fig. 1 or 9) or EMII and DMM (Fig. 10 or 11). This doesn't mean mixing between these components is non-existent, as curved arrays would be very hard to extract from this kind of data. What is obvious from Fig. 9 and 11, however, is that the EMII islands do show very elongated and linear-appearing arrays which are not obviously headed toward any of the other end-members. For example, in Fig. 11, the arrays from EMII are more or less vertical, (constant $^{206}Pb/^{204}Pb$), and if they represent mixing arrays to either DMM or HIMU, the Nd/Pb (or Sr/Pb) ratio in EMII must be much lower than in DMM or HIMU to produce arrays with very marked concave up curvature. The Marquesas array in Fig. 11 in fact shows such a sharp curve toward HIMU, but in detail this relationship is not particularly consistent on other plots (especially Fig. 9).

Another "view" of these EMII arrays is provided by Fig. 15, which displays the Nd deviation from the mantle plane versus $^{87}Sr/^{86}Sr$ (see Fig. 7 for the total data set in this representation). What is remarkable about the "EMII anchored" arrays is their large range and approximate co-linearity. None of the other three components serve as starting points for arrays which traverse such a large range in Sr and Nd (this effect is also

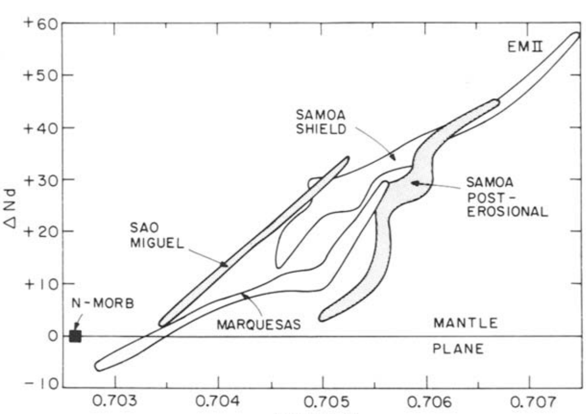

Fig. 15. ΔNd versus $^{87}Sr/^{86}Sr$ correlation plot for islands showing dominant EMII signatures; ΔNd is defined in Fig. 6 caption.

striking in Fig. 9 and 11). On the other hand, these EMII-based arrays show relatively little dispersion on the Pb-Pb plots. Figs. 7 and 15 further emphasize the apparent lack of linear arrays between EMII and the other components. Thus, EMII contrasts significantly from the other components —it doesn't show linear mixing with them, when present it generates extreme variations in Sr and Nd but limited variations in Pb, and it tends always to mix toward some intermediate composition in isotopic space (so all EMII-originated arrays end up more or less co-linear). These observations suggest a few speculations: (1) the Pb/Sr and Pb/Nd ratio in EMII is much higher than in the other components, leading to markedly curved, "Pb-dominated" arrays (on plots such as Figs. 10 and 11); (2) the Sr/Nd ratio in EMII is similar to that in DMM, at least (Fig. 9); (3) the EMII end member is not very different in Pb isotopic signature from the extreme OIB samples; however, the Sr and Nd isotopic ratios are well removed from the OIB field, leading to large variations in Sr and Nd.

7. Generation of mantle components

To this point, I have been describing isotopic relationship in oceanic mantle, cataloguing components, and qualitatively discussing interactions of these components. I have deferred any genetic discussion until this descriptive format was stitched together. I will now address the fundamental questions of how these various components originated, and where they are currently situated in the mantle.

7.1. The DMM component

Because it is sampled, in some sense passively, by the world-wide spreading ridge system, the depleted MORB mantle must reside in the uppermost mantle; there is little or no argument on this point. This mantle is depleted in LIL (large-ion lithophile) or incompatible elements, and most would agree that the missing budget of these elements is now largely resident in the continental crust. The exact pathways by which these elements have migrated from the upper mantle into the crust is a contentious issue; it probably involves both melt removal processes occurring at spreading centers, and melt-fluid extraction processes occurring in subduction zones. Also contentious is the issue of whether the depleted MORB mantle should be defined as an extreme end-member, or as the average of N-type MORB [67]. In one case, the processes which depleted the upper mantle may have done so at different times and with different efficiencies, leaving a mantle with significant "primary" heterogeneity; in this case, the average of all N-MORB would be the best representation of this reservoir. In the alternative case, the upper mantle may have been fairly uniformly and highly depleted, and is best represented by the most extreme MORB samples available; all other MORB, then, would represent pollution or contamination of this extreme DMM reservoir with other more enriched components. In regions adjacent or contiguous to hot spots, this contamination process is clear and unequivocal (e.g., Iceland [68]); and leads to identifiably contaminated MORB (P-type MORB). It is possible that average N-MORB is simply a mild and unrecognizable result of this same process. More extended discussion of these questions may be found in White et al. [31] and Ito et al. [32]. While these questions are important, the fact remains that we know much more about the DMM components than we do about any of the other components; these DMM issues are not presently crippling our forward progress.

7.2. The HIMU component

A variety of origins has been proposed for this component, ranging from extraction of Pb into the core [64–66], to recycling of ancient altered oceanic crust [22,69,70], to recycling of ancient continental crust [21], to intra-mantle metasomatism [20,54]. Probably none of these models can be apodictically ruled out at this point.

Core pumping of Pb is out of favor, because the HIMU component falls well to the right of the geochron (core accretion is completed early in earth history [71]; HIMU appears younger than this). However, it seems premature to me to exclude possible long-term chemical and physical interactions between the core and mantle, which could serve to develop a HIMU component in a core/mantle boundary layer. Based on the evidence discussed earlier for similar Nd/Pb and Sr/Pb in HIMU, DMM and EMI, it would seem that U enrichment, not Pb depletion, is characteristic of HIMU and therefore core pumping of Pb is not appropriate. Arguments against core pumping based on siderophile and chalcophile element abundances in oceanic basalts are also quite convincing [37].

Analytical estimates of the composition of altered oceanic crust have been made by Hart and Staudigel [72], and these strongly prohibit identification of HIMU directly with this material. The problem is that altered oceanic crust is characterized by high Rb/Sr (~ 0.1), high U/Pb (~ 50) and low Th/U (~ 0.22); subduction and aging of this material will lead to high $^{206}Pb/^{204}Pb$, to be sure, but this will be accompanied by high $^{87}Sr/^{86}Sr$ and low $^{208}Pb/^{206}Pb$, neither of which is characteristic of HIMU (note that HIMU does fall below the NHRL on $^{208}Pb/^{204}Pb$–$^{206}Pb/^{204}Pb$, Fig. 3; however, with a Th/U of only 0.22, old oceanic crust would have $^{208}Pb/^{204}Pb$ ratios *less than* the lowest values in the OIB data set!).

The problem is not quite so clear-cut, however, with the realization that oceanic crust probably does not pass through the subduction "processing zone" without modification [22]. In the process of dehydration and transformation into eclogite, major chemical modifications will occur [73], and it is impossible to tell at this point what the trace element composition of the final recycled ocean crust product might be. The process of seawater alteration of oceanic crust is one which significantly enhances Rb and U without affecting Sr, Nd or Pb concentrations appreciably. Thus the relative abundances of Sr, Nd and Pb are preserved during alteration, and this is consistent with the requirement derived from the linear DMM–HIMU array (No-Em array). Subsequent modification during subduction-zone processing thus needs to remove Rb, relative to U, without strongly perturbing these Sr, Nd, Pb relationships. It has been shown [28] that HIMU basalts do have unusually low Rb/Nb ratios, relative to EM basalts, and that the trace element patterns of HIMU basalts are a mirror image of island arc basalts [41]. These authors [28,41] therefore argue that subducted altered, oceanic crust is the source for the HIMU basalts, but only after significant modification during subduction zone processing.

Other recycled materials (continental crust/sediment) are also clearly not suitable as protoliths for HIMU unless similarly ad-hoc chemical manipulations are performed during processing through subduction zones. The only argument which might be made against ad-hoc processes of this magnitude is to ask where this "removed" material is going; if being introduced into the mantle wedge above subducting plates, why don't arc magmas show opposing Rb and U anomalies?

Identification of HIMU with a metasomatic process [54] was based on the connection between HIMU and EMI implied by the LoNd array, and by a virtual failure of other possible explanations. I will therefore defer discussion of a metasomatic origin of HIMU pending the following discussion of EMI.

7.3. The EMI component

In their original discussion of the Walvis Ridge data, Richardson et al. [51] favored derivation of these basalts from a mantle which had been "enriched" by small volume melts and metasomatic fluids. The enrichment event was assigned a minimum age of ~ 800 m.y., and speculatively associated with sub-continental African lithospheric events related to intra-continental tectonics. While Richardson et al. [51] didn't specify what kind of mantle protolith was being metasomatized, the most striking characteristic of EMI is that it is the closest to "bulk earth" isotopically, of the four mantle components. Hart et al. [54] showed by a simple model calculation that EMI could be derived from bulk earth 2 b.y. ago, for example, by very minor changes in parent/daughter element ratios (increase Rb/Sr by 12% and decrease Sm/Nd by 10%, U/Pb by 6% and Th/Pb by 1%). Viewed in this light, I would choose to assert that EMI is slightly modified primitive or bulk-earth mantle, rather than ascribe its origin to other more exotic protoliths (e.g., recycled oceanic crust or sediment) where it is difficult to avoid much larger variations in these trace element ratios.

Insofar as the relative abundances of Sr, Nd and Pb in EMI can be linked to those in HIMU through the linearity of the LoNd array, and similarly those in HIMU can be linked to DMM through the No-Em array, then all three components should have approximately bulk-earth proportions of Sr, Nd and Pb. This can be supported to some extent by direct observation of Sr, Nd and Pb abundances in MORB and basalts from HIMU islands (Pb concentration data for Walvis Ridge basalts are lacking). Sr/Nd in bulk earth and in DMM was estimated at 16.4 and 16.6 respectively [20]; in Walvis (EMI) basalts, it is 11.9, in St. Helena and Mangaia (HIMU) basalts, it is 13.6. Nd/Pb in bulk earth and DMM was estimated at 7.6 and 14.3 [20]; in HIMU basalts, it is 16.3. Taking basalt trace element ratios as indicative of mantle source ratios is, of course, fraught with difficulties, especially for alkali basalts. Tholeiites, especially MORB, are usually considered to closely reflect their mantle source in most LIL element ratios; some caveat may be needed here, in light of proposals that even MORB sources may undergo metasomatic enrichment prior to [74] or during upwelling and melting [75]. In any event, the proposition that EMI, HIMU and DMM have similar relative abundances of Sr, Nd and Pb will be taken as a reasonable working hypothesis. Relative to bulk earth, then, the HIMU source has been depleted in Rb by a factor of 5, and enriched in Sm, U and Th by 9%, 114% and 61% respectively. These are rather major fractionations, with, for example, U/Rb being enriched by a factor of 10 [54], relative to bulk earth.

Hart et al. [54] discussed the role of phlogopite as a potential U/Rb fractionating phase during a metasomatic process and concluded that it might be suitable. Roden [76] considered two actual suites of metasomatic mantle rocks (Nunivak and St. Paul's Rocks), and argued that aging of this material would produce a low Nd-low Sr isotopic source (EMI-like, and not appropriate for EMII). This discussion, plus the observation that the U/Rb ratios of the metasomatic material from St. Paul's Rocks is much lower than bulk earth (~ 0.01 versus ~ 0.04; S.R. Hart unpublished data), would seem to rule out this particular type of metasomatized rock as a candidate for HIMU. However, the distinctive feature of both the Nunivak and St. Paul's suites is the presence of amphibole, not phlogopite, as the dominant metasomatic phase. As cogently argued by Hawkesworth et al. [88], there are several types of metasomatic processes operating in the lithosphere; depending on whether the metasomatizing agent is silicate melt or fluid, and CO_2 or H_2O rich, metasomatism will lead to different phase assemblages and consequent differences in trace element fractionations.

The most reasonable hypothesis, at this stage, is to assign a metasomatic origin to HIMU; indeed, there seems no other viable model. For EMI, since it is only slightly modified bulk earth, a metasomatic process is also appealing and, as noted by Hart et al. [54], EMI and HIMU may be complementary parts of the same metasomatic process (infiltrate versus residue). Discussion of the present location of these components, or of the metasomatic process, will be deferred until EMII is discussed.

7.4. The EMII component

The most common model for EMII (or enriched components in general) specifies them as subducted and recycled continental material [21,77,78]. This is an appealing model for several reasons: (1) the isotopic characteristics of continentally-derived sediment are ideal for an EMII component ($^{87}Sr/^{86}Sr > 0.710$, $^{143}Nd/^{144}Nd < 0.5120$, limited range of $^{206}Pb/^{204}Pb = 18.5–19.2$); (2) in island arcs where sediment subduction and contamination of arc lavas is strongly implicated (e.g., Banda, Antilles), the resulting isotopic signatures bear a strong kinship with those of the EMII oceanic basalts.

For both terrigenous oceanic sediments [79] and clay-rich pelagic sediments (S.R. Hart, unpublished data), Sr/Pb and Nd/Pb concentration ratios are a factor of 10–40 lower than bulk earth or MORB and Sr/Nd ratios are similar to or lower by up to a factor of 3 (depending on carbonate content). This means that mixing arrays between DMM (or bulk earth) and sediment will show little to mild concave-up curvature on Nd-Sr isotope plots, and very strong to almost right-angle curvature on Sr-Pb (or Nd-Pb) plots. This is totally consistent with the sense of curvature noted for the EMII arrays in Figs. 9, 10, 11 and 15. Furthermore, in the case of Sr and Nd, the sediments have isotopic ratios well removed from even the most extreme EMII samples, while the sediment Pb ratios are very close to the extreme EMII samples; this serves nicely to explain why the EMII arrays for Sr and Nd are very large in extent whereas the Pb-Pb arrays are very limited in extent.

In looking at Fig. 4, one sees that the EMII array is not directed at the terrigenous sediment field and only grazes the lower side of the pelagic field; it might also be mentioned that the field of world-wide arc volcanics overlaps that for OIB at low ΔPb values, and extends up and well into the pelagic sediment field. I interpret this to mean that young sediments are a component in many arcs, but that the sediment component involved in EMII has aged for some significant period of time. Because oceanic sediments have low U/Pb ratios and high Th/U ratios (typically 0.04–0.09 and 5–10, respectively), a few hundred million years of aging will suffice to mildly increase $\Delta 7/4$ Pb and strongly increase $\Delta 8/4$ Pb, allowing the sediment field to "overtake" the EMII sample arrays on this plot (Fig. 4). By the same token, it is unlikely that truly ancient recycled sediment is involved in EMII, because the $^{206}Pb/^{204}Pb$ ratio would lag much too far behind—as it is, the EMII arrays, with $^{206}Pb/^{204}Pb$ of 18.7–19.2, are on the high side of pelagic sediment leads (18.6–19.0); they are comfortably on the low side of terrigenous sediments, however (18.8–19.8). The young "recycling" age required for the sediment also implies that it will not have travelled far from the injection site, and it will not have had time to lose its identity by stirring in the upper MORB mantle.

8. Where is home?

For DMM, the answer is clear—the upper mantle is home (though arguments exist as to whether this means the upper 500 km or the upper 1000 km). For a sediment-based EMII, as just discussed, long-term storage is contra-indicated, so old subcontinental lithosphere or a core/mantle boundary layer seem unlikely. Short-term storage in a mesosphere boundary layer as advocated by Allègre and Turcotte [21] is certainly a possibility.

If EMI is a slightly modified bulk-earth component, it clearly needs to be stored out of the upper mantle circulation for a long time. This can be done in the subcontinental lithosphere, in the deep mantle, or in a core/mantle boundary layer. Hart et al. [54] advocated a subcontinental lithospheric home, because this is clearly capable of long-term storage [80], and because the connection with HIMU, and its metasomatic imprint, seemed best accomplished in the lithosphere (for example, during exposure to subjacent slab dewatering, or during long-term catching of blobs and weak plumes [14]. However, the deeper mantle is clearly not totally degassed [106], and volatiles may undergo periodic trapping and release during phase transformations in the transition region of the mantle. This action could generate a localized "auto-metasomatism" which could be very effective in producing a HIMU–EMI complementary "metasomatic pair" (the evidence from the LoNd array suggests these two components are commonly spatially contiguous). At the same time, the evidence from the No-Em array suggests that HIMU is frequently available for "pure" mixing with DMM; this suggests that EMI and HIMU are not an inseparable duo.

If EMI and HIMU *are* stored in the subcontinental lithosphere, then it should be possible to find evidence for this either in lithospheric xenoliths, or in basalts which initiate in, or interact with, lithosphere during ascent. As shown in fig. 1 of Zindler and Hart [20], xenoliths from both kimberlite and alkali basalt hosts frequently show an EMI signature in Sr and Nd isotopes; there are also HIMU-like xenoliths reported. I have compiled what Pb data are available on xenoliths and show this in Fig. 16. Also shown on this plot are continental basalts which carry xenoliths (as a possible filter against crustal contamination effects). What is striking about this plot is the complete absence of data in either the EMI or DMM areas; while there are also no HIMU data shown in this figure, several mafic layers from the Ronda peridotite massif have been analyzed (MIT) with $^{206}Pb/^{204}Pb$ in the range 20.2–21.7. While much of the data does fall within the limits of the OIB field, there are clearly numerous outliers as well. There is a significant clustering of data in the $^{206}Pb/^{204}Pb$ range from 18.5 to 19.5, and while

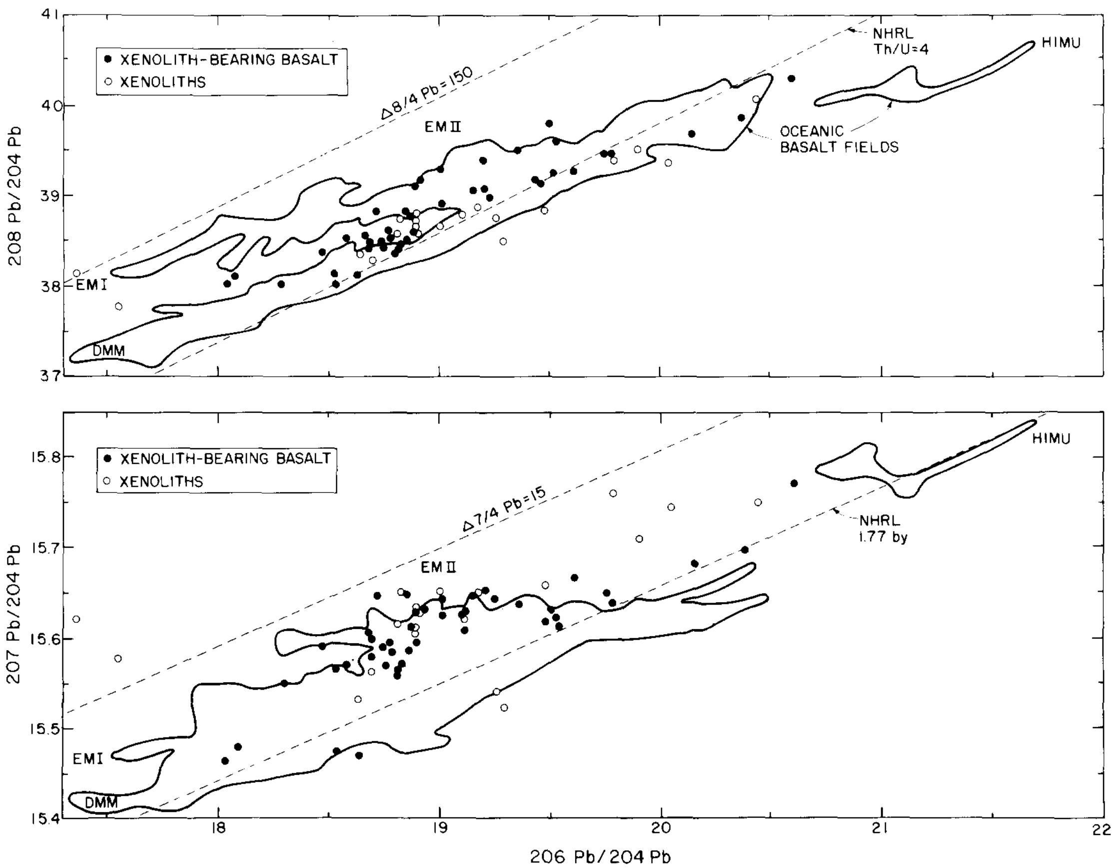

Fig. 16. Pb-Pb isotope correlation plot for ultramafic xenoliths (open symbols) and xenolith-bearing basalts (solid symbols) from continental areas. Most of the xenolith data are from Kramers et al. [95] and Cohen et al. [96]; most of the basalt data are unpublished MIT data (remainder from Alibert et al. [97]; Allègre et al. [98]; Worner et al. [99]). Fields enclose the total observed range of all oceanic basalts, MORB included. Northern hemisphere reference line (NHRL) and two DUPAL anomaly Pb reference lines ($\Delta 7/4$ Pb = 15, $\Delta 8/4$ Pb = 150) are as defined by Hart [7].

this cluster shows the high $^{207}Pb/^{204}Pb$ signature of EMII, the $^{208}Pb/^{204}Pb$ is less obviously like EMII. On a delta–delta Pb plot (such as Fig. 4), this cluster of data would fall outside the OIB field and close to the pelagic sediment field—i.e., this particular set of continental basalt and xenolith data are very much like many arc volcanics which have a sediment component. This might suggest that much of the subcontinental lithosphere, during its accretion history, has been impregnated from subjacent subduction with slab-derived fluids carrying a sediment Pb signature. In any event, DMM and EMI are not present in the existing data set. In a pioneering study, the Paris group have reported that the whole range of oceanic Pb's can be found in a single ultramafic massif [56], but specific data aren't given to know whether this includes EMI, for example.

It is clearly premature, based on the existing data set, to say that the EMI component is absent from the subcontinental lithosphere; an EMII-like component is clearly present, as is at least one example of HIMU (Ronda). Assuming EMI can be found in subcontinental lithosphere, then the whole oceanic mantle story can be reconciled without ever digging deeper than a few hundred kilometers.Delamination of continental lithosphere [81] and entrainment in the upper DMM circulation provides all the necessary OIB components; their survival time need not be long, because a fresh supply of aged lithosphere is always near at hand.

The principal difficulty in my mind with this very simple model is how then to explain the DUPAL anomaly? The sub-equatorial restriction of the DUPAL would argue that delamination of subcontinental lithosphere and sediment injection was also restricted to this sub-equatorial belt. Allègre and Turcotte [21] suggest exactly this, with Pangean collisions and peri-Pangean subduction zones being concentrated in the DUPAL belt during the period 400 to 150 m.y. ago. This seems a little too pat to me—what about the closing and opening of North America and Europe? Why didn't this leave Proterozoic lithosphere floating around? What about the Pacific subduction zones in the northern hemisphere? There is no EMII component whatsoever at Nunivak.

There is an interesting similarity between the DUPAL and several other geophysical anomalies which are also dominated by low-degree harmonics with equatorial placement. The slab-corrected geoid, for example, is dominated by two equatorial highs located in the westernmost and easternmost Pacific [82]. This quadrupolar pattern is mirrored in the deepest mantle P-wave tomographic maps [83]. Creager and Jordan [84] show two large slow P-wave regions at the core/mantle boundary, one southwest of Australia and one west of South America (both, like the DUPAL, lying some 30–40° south of the equator). And in the core itself, Le Mouel et al. [85] show two equatorial anomalies: one an upwelling, and one a downwelling, both approximately antipodal to each other. And of course the density of hotspots on the earth is not uniform, but shows a significant concentration toward low latitudes [86]. While the exact "positions" of these various anomalies are not all coincident, they are all characterized by low-degree antipodal features lying close to an equatorial plane. The DUPAL is also close to equatorial, and marked by two highs. The seismic anomalies and the core motion anomalies are clearly deep-seated features; the low degree geoid feature is also arguably deep-rooted.

As a speculative alternative to the mesosphere boundary layer model of Allègre and Turcotte [21], I propose that the EMI and HIMU components are metasomatic in origin and are stored in the core/mantle boundary layer (CMBL—the "continents on the core" of Creager and Jordan [84]); that the low-degree general mantle circulation is one of whole mantle equatorial upwelling and polar downwelling; and that the DUPAL hotspots are fed from instabilities on the CMBL and these are concentrated in equatorial regions by thermal coupling to the heat loss from the core and by "sweeping together" in the large-scale flow; the absence of DUPAL signatures outside the DUPAL belt is a result of diapirs originating in the CMBL at non-equatorial locations having to travel a greater distance and be subject to greater shear strain mixing with the DMM during travel through the large-scale quadrupolar circulation.

9. Looking ahead

Certainly, the first-order isotopic mapping job is far from done; comprehensive Sr-Nd-Pb (and rare gas) data sets are needed from as many islands as possible, and in particular those islands where large intra-island variations are already known. The challenge here is to convince ourselves that four principal components are enough, and to try to better define both the homogeneity of these components and the nature of the mixing arrays between components. The natural lack of polar hotspots will perhaps need to be addressed by carrying out particularly detailed studies on the ones that do exist. With the advent of multi-collector mass spectrometers, the OIB work will not be rate-limited by analytical capability, but by how rapidly geologically well-documented field sample collections can be attained.

Beyond the oceanic work, we need a major effort on the subcontinental lithosphere because, along with MORB, it is the only mantle reservoir whose location we can be sure of. The challenge here is to generate both Sr-Nd *and Pb* data on the same samples; while continental basalts may carry some information from the lithosphere, it will always be somewhat equivocal to interpret. Direct analysis of ultramafic material is to be preferred by far, of both erupted xenoliths and ultramafic massifs. This work will either demonstrate the presence of all necessary OIB components in the subcontinental lithosphere or it won't. The final understanding of where the oceanic mantle components come from and how they move about and interact will depend on integrating all of the geochemical data with high-resolution 3-D mantle seismic tomography, since geochemistry by itself has little or no depth resolution (beyond a few hundred kilometers).

Acknowledgements

I greatly appreciate the many people who provided samples for analysis (Tony Erlank for Marion/Prince Edward, Mike Roden for Koolau and Nunivak, Mike Rabinowitz for Ponape, Jim Cole for Balleny, John Campsie for Scott, Bruce Tomich for Christmas and Brent Dalrymple for La Perouse Pinnacles). Also, thanks to Mike Roden for the unpublished Sr and Nd data for Nunivak, and thanks to Julie Morris and Levent Gulen for help with many of the isotopic analyses. I and my data-hungry spreadsheet are also grateful to Alan Zindler, Dave Graham, Tatz, Dave Gerlach and Bob Cliff for numerous preprints full of numbers. Diane Watson-Mitchell spent much of the holiday season preparing the manuscript—thank you, Santa. I am grateful to NSF for their long-term support, via EAR 8308809 and EAR 8708372. And, as always, Ken Burrhus kept the mass spectrometers purring by always knowing which corner to kick, and how big a hammer to use. And finally, I wish to express my congratulations to, and my appreciation of, the 1986 Crafoord laureates—to Jerry Wasserburg for kindling an isotopic fire in me as a graduate student, and to Claude Allègre for stoking the fire over 20 years of friendship.

References

1 G. Faure and P.M. Hurley, The isotopic composition of strontium in oceanic and continental basalt: application to the origin of igneous rocks, J. Petrol. 4, 31–50, 1963.
2 C.E. Hedge and F.G. Walthall, Radiogenic strontium-87 as an index of geological processes, Science 140, 1214–1217, 1963.
3 P.W. Gast, G.R. Tilton and C. Hedge, Isotopic composition of lead and strontium from Ascension and Gough Islands, Science 145, 1181–1185, 1964.
4 M. Polvé and C.J. Allègre, Orogenic lherzolite complexes studied by ^{87}Rb-^{87}Sr: a clue to understand the mantle convection processes?, Earth Planet. Sci. Lett. 51, 71–93, 1980.
5 L. Reisberg and A. Zindler, Extreme isotopic variability in the upper mantle: evidence from Ronda, Earth Planet. Sci. Lett. 81, 29–45, 1986.
6 B. Dupré and C.J. Allègre, Pb-Sr isotope variation in Indian Ocean basalts and mixing phenomena, Nature 303, 142–146, 1983.
7 S.R. Hart, A large-scale isotope anomaly in the Southern Hemisphere mantle, Nature 309, 753–757, 1984.
8 M. Tatsumoto, Isotopic composition of lead in oceanic basalt and its implication to mantle evolution, Earth Planet. Sci. Lett. 38, 63–87, 1978.
9 D.J. DePaolo and G.J. Wasserburg, Inferences about magma sources and mantle structure from variations of ^{143}Nd/^{144}Nd, Geophys. Res. Lett. 3, 743–746, 1976.
10 S.-S. Sun, Lead isotopic study of young volcanic rocks from midocean ridges, ocean islands and island arcs, Philos. Trans. R. Soc. London, Ser. A 297, 409–445, 1980.
11 P.J. Patchett and M. Tatsumoto, Hafnium isotope variations in oceanic basalts, Geophys. Res. Lett. 7; 1077–1080, 1980.
12 M. Tatsumoto, Genetic relations of oceanic basalts as indicated by lead isotopes, Science 153, 1094–1101, 1966.
13 P.W. Gast, The isotopic composition of lead from St. Helena and Ascension Islands, Earth Planet. Sci. Lett. 5, 353–359, 1969.

14 C. Brooks, S.R. Hart, A.L. Hofmann and D.E. James, Rb-Sr mantle isochrons from oceanic regions, Earth Planet. Sci. Lett 32, 51–61, 1976.
15 C.E. Hedge and Z.E. Peterman, The strontium isotopic composition of basalts from the Gordo and Juan de Fuca Rises, Northeastern Pacific Ocean, Contrib. Mineral. Petrol. 27, 114–120, 1970.
16 S.R. Hart, K, Rb, Sc, Sr and Ba contents and Sr isotope ratios of ocean floor basalts, Philos. Trans. Roy. Soc. London, Ser A 26, 573–587, 1971.
17 C.J. Allègre, Chemical geodynamics, Tectonophysics, 81, 109–132, 1982.
18 G.F. Davies, Geophysical and isotopic constraints on mantle convection: an interim synthesis, J. Geophys. Res. 89, 6017–6040, 1984.
19 D.L. Anderson, Isotopic evolution of the mantle: a model, Earth Planet. Sci. Lett. 57, 13–24, 1982.
20 A. Zindler and S. Hart, Chemical geodynamics, Annu. Rev. Earth Planet.Sci. 14, 493–571, 1986.
21 C.J. Allègre and D.L. Turcotte, Geodynamic mixing in the mesosphere boundary layer and the origin of oceanic islands, Geophys. Res. Lett. 12, 207–210, 1985.
22 A. Zindler, E. Jagoutz and S. Goldstein, Nd, Sr and Pb isotopic systematics in a three-components mantle: a new perspective, Nature 58, 519–523, 1982.
23 D.W. Graham, A. Zindler, M.D. Kurz, W.J. Jenkins, R. Batiza and H. Staudigel, Helium, lead, strontium and neodymium isotope constraints on magma genesis and mantle heterogeneity beneath young Pacific seamounts, Contrib. Miner. Petrol. 99, 446–463, 1988.
24 D.C. Gerlach, R.A. Cliff, G.R. Davies, M. Norry and N. Hodgson, Magma sources of the Cape Verdes Archipelago: isotopic and trace element constraints, Geochim. Cosmochim. Acta, in press, 1988.
25 D.C. Gerlach, J.C. Stormer, Jr. and P.A. Mueller, Isotopic geochemistry of Fernando de Noronha, Earth Planet. Sci. Lett. 85, 129–144, 1987.
26 H.B. West, D.C. Gerlach, W.P. Leeman, and M.O. Garcia, Isotopic constraints on the origin of Hawaiian lavas from the Maui Volcanic Complex, Hawaii, Nature 330, 216–220, 1987.
27 H.B. West and W.P. Leeman, Isotopic evolution of lavas from Haleakala Crater, Hawaii, Earth Planet. Sci. Lett. 84, 211–225, 1987.
28 Z.A. Palacz, and A.D. Saunders, Coupled trace element and isotope enrichment in the Cook-Austral-Samoa islands, southwest Pacific, Earth Planet. Sci. Lett. 79, 270–280, 1986.
29 E. Wright and W.M. White, The origin of Samoa: new evidence from Sr, Nd, and Pb isotopes, Earth Planet. Sci. Lett. 81, 151–162, 1987.
30 D.J. Chaffey, R.A. Cliff and B.M. Wilson, Characterization of the St. Helena magma source, J. Geol. Soc. London, in press, 1988.
31 W.M. White A.W. Hofmann and H. Puchelt, Isotope geochemistry of Pacific mid-ocean ridge basalt, J. Geophys. Res. 92, 4881–4893, 1987.
32 E. Ito, W.M. White, and C. Göpel, The O, Sr, Nd, and Pb isotope geochemistry of MORB, Chem. Geol. 62, 157–176, 1987.
33 R.A. Duncan, M.T. McCulloch, H.G. Barsczus and D.R. Nelson, Plume versus lithospheric sources for melts at Ua Pou, Marquesas Islands, Nature 322, 534–538, 1986.
34 S.B. Shirey, J.F. Bender and C.H. Langmuir, Three-component isotopic heterogeneity near the Oceanographer transform, Mid-Atlantic Ridge, Nature 325, 217–223, 1987.
35 Q. Cheng, K.-H. Park, J.D. Macdougall, A. Zindler, G.W. Lugmair, H. Staudigel, J. Hawkins and P. Lonsdale, Isotopic evidence for a hotspot origin of the Louisville seamount chain, in: Seamounts, Islands and Atolls, B.H. Keating, P. Fryer, R. Batiza and G.W. Boehlert, eds., Am. Geophys. Union, Geophys. Monogr. 43, 283–296, 1988.
36 G.R.Davies, M.J. Norry, D.C. Gerlach and R.A. Cliff, A combined chemical and Pb-Sr-Nd isotope study of the Azores and Cape Verde hot spots: the geodynamic implications, J. Geol. Soc. London, in press, 1988.
37 H.E. Newsom, W.M. White, K.P. Jochum and A.W. Hofmann, Siderophile and chalcophile element abundances in oceanic basalts, Pb isotope evolution and growth of the Earth's core, Earth Planet. Sci. Lett. 80, 299–313, 1986.
38 D.J. Geist, W.M. White and A.R. McBirney, Plume-asthenosphere mixing beneath the Galapagos Archipelago, in press, 1988.
39 D. Weis, Pb isotopes in Ascension Island rocks: oceanic origin for the gabbroic to granite plutonic xenoliths, Earth Planet. Sci. Lett. 62, 273–282, 1983.
40 D. Weis, D. Demaiffe, S. Cauet and M. Javoy, Sr, Nd, O and H isotopic ratios in Ascension Island lavas and plutonic inclusions; cogenetic origin, Earth Planet. Sci. Lett. 82, 255–268, 1987.
41 C. Dupuy, P. Vidal, H.G. Barsczus and C. Chauvel, Origin of basalts from the Marquesas Archipelago (south central Pacific Ocean): isotope and trace element constraints, Earth Planet. Sci. Lett. 82 145–152, 1987.
42 E. Hegner, D. Unruh and M. Tatsumoto, Nd-Sr-Pb isotope constraints on the sources of West Maui volcano, Hawaii, Nature 319, 478–480, 1986.
43 P. Stille, D.M. Unruh and M. Tatsumoto, Pb, Sr, Nd and Hf isotopic constraints on the origin of Hawaiian basalts and evidence for a unique mantle source, Geochim. Cosmochim. Acta 50, 2303–2319, 1986.
44 M. Tatsumoto, E. Hegner and D.M. Unruh, Origin of the West Maui volcanics inferred from Pb, Sr, and Nd isotopes and a multi-component model for oceanic basalts, U.S. Geol. Surv., Prof. Pap. 1350, 723–744, 1987.
45 R.C. Price, A.K. Kennedy, M. Riggs-Sneeringer and F.A. Frey, Geochemistry of basalts from the Indian Ocean triple junction: implications for the generation and evolution of Indian Ocean ridge basalts, Earth Planet. Sci. Lett. 78, 379–396, 1986.
46 A. Michard, R. Montigny and R. Schlich, Geochemistry of the mantle beneath the Rodriguez Triple Junction and the South-East Indian Ridge, Earth Planet. Sci. Lett. 78, 104–114, 1986.
47 B. Hamelin, B. Dupré and C.J. Allègre, Pb-Sr-Nd isotopic data of Indian Ocean ridges: new evidence of large-scale mapping of mantle heterogeneities, Earth Planet. Sci. Lett. 76, 288–298, 1986.
48 H. Staudigel, A. Zindler, S.R. Hart, T. Leslie, C.-Y. Chen and D. Clague, The isotope systematics of a juvenile intraplate volcano: Pb, Nd and Sr isotope ratios of basalts

from Loihi Seamount, Hawaii, Earth Planet. Sci. Lett. 69, 13–29, 1984.

49 B.D. Taras and S.R. Hart, Geochemical evolution of the New England seamount chain: isotopic and trace-element constraints, Chem. Geol. 64, 35–54, 1987.

50 D.C. Gerlach, S.R. Hart, V.W.J. Morales and C. Palacios, Mantle heterogeneity beneath the Nazca plate: San Felix and Juan Fernandez islands, Nature 322, 165–169, 1986.

51 S.H. Richardson, A.J. Erlank, A.R. Duncan and D.L. Reid, Correlated Nd, Sr and Pb isotope variation in Walvis Ridge basalts and implications for the evolution of their mantle source, Earth Planet. Sci. Lett. 59, 327–342, 1982.

52 W.M. White, Sources of oceanic basalts: radiogenic isotopic evidence, Geology 13, 115–118, 1985.

53 C.J. Allègre, B. Hamelin, A. Provost and B. Dupré, Topology in isotopic multispace and origin of mantle chemical heterogeneities, Earth Planet. Sci. Lett. 81, 319–337, 1987.

54 S.R. Hart, D.C. Gerlach and W.M. White, A possible new Sr-Nd-Pb mantle array and consequences for mantle mixing, Geochim. Cosmochim. Acta 50, 1551–1557, 1986.

55 Y. Nakamura and M. Tatsumoto, Is mantle plume homogeneous? Pb, Nd, Sr isotopic evidence for multi-component source for Cook-Austral island rocks, Geochim. Cosmochim. Acta, in press, 1988.

56 B. Hamelin and C.J. Allègre, Large scale regional units in the depleted upper mantle revealed by an isotopic study of the Southwest Indian Ridge, Nature 315, 196–199, 1985.

57 W.M. White and A.W. Hofmann, Sr and Nd isotope geochemistry of oceanic basalts and mantle evolution, Nature 296, 821–825, 1982.

58 Ph. Vidal, C. Chauvel and R. Brousse, Large mantle heterogeneity beneath French Polynesia, Nature 307, 536–538, 1984.

59 S.E. Church and M. Tatsumoto, Lead isotope relations in oceanic ridge basalts from the Juan de Fuca–Gorda Ridge area, NE Pacific Ocean, Contrib. Mineral. Petrol. 53, 253–279, 1975.

60 C.J. Allègre, B. Dupré, A.V. Sobolev and L.N. Kogarko, The Asian province in OIB cartography, EOS 68, 1529, 1987.

61 H. Staudigel, K.-H. Park, M. Pringle and A. Zindler, Tracing the South Pacific isotopic anomaly back in time, EOS 68, 1445, 1987.

62 K. Futa and W.E. Le Masurier, Nd and Sr isotopic studies on Cenozoic mafic lavas from west Antarctica: another source for continental alkali basalts, Contrib. Mineral. Petrol. 83, 38–44, 1983.

63 A. Zindler, S.R. Hart, F.A. Frey and S.P. Jakobsson, Nd and Sr isotope ratios and rare earth element abundances in Reykjanes Peninsula basalts; evidence for mantle heterogeneity beneath Iceland, Earth Planet. Sci. Lett. 45, 249–262, 1979.

64 R. Vollmer, Terrestrial lead evolution and formation time of the Earth's core, Nature 270, 144–147, 1977.

65 P. Vidal and L. Dosso, Core formation: catastrophic or continuous? Sr and Pb isotope geochemistry constraints, Geophys. Res. Lett. 5, 169–172, 1978.

66 C.J. Allègre, O. Brevart, B. Dupré and J.-F. Minster, Isotopic and chemical effects produced in a continuously differentiating convecting Earth mantle, Philos. Trans. R. Soc. London, Ser. A 297, 447–477, 1980.

67 C.J. Allègre, S.R. Hart and J.-F. Minster, Chemical structure and evolution of the mantle and continents determined by inversion of Nd and Sr isotopic data, II. Numerical experiments and discussion, Earth Planet. Sci. Lett. 66, 191–213, 1983.

68 S.R. Hart, J.-G. Schilling and J.L. Powell, Basalts from Iceland and along the Reykjanes Ridge: Sr isotopic geochemistry, Nature Phys. Sci. 246, 104–107, 1973.

69 C.G. Chase, Ocean island Pb: two-stage histories and mantle evolution, Earth Planet. Sci. Lett. 52, 277–284, 1981.

70 A.W. Hofmann and W.M. White, Mantle plumes from ancient oceanic crust, Earth Planet. Sci. Lett. 57, 421–436, 1982.

71 D.J. Stevenson, Models of the Earth's core, Science 214, 611–619, 1981.

72 S.R. Hart and H. Staudigel, Isotopic characterization and identification of recycled components, in: Crust/Mantle Recycling at Convergence Zones, L. Gulen and S.R. Hart, eds., NATO ASI Ser., in press, D. Reidel, Dordrecht, 1988.

73 A. Zindler and E.B. Watson, Chemical fluxes associated with dewatering during subsolidus recrystallization of hydrous basalt, in: Crust/Mantle Recycling at Convergence Zones, L. Gulen and S.R. Hart, eds., NATO ASI Ser., in press, D. Reidel, Dordrecht, 1988.

74 M.K. Roden, S.R. Hart, F.A. Frey and W.G. Melson, Sr, Nd and Pb isotopic and REE geochemistry of St. Paul's Rocks: the metamorphic and metasomatic development of an alkali basalt mantle source, Contrib. Mineral Petrol. 85, 376–390, 1984.

75 S.J.G. Galer and R.K. O'Nions, Magmagenesis and the mapping of chemical and isotopic variations in the mantle, Chem. Geol. 56, 45–61, 1986.

76 M.F. Roden, Rb/Sr and Sm/Nd ratios of metasomatized mantle; implications for the role of metasomatized mantle in the petrogenesis of Na_2O-rich alkaline basalts, Geol. Soc. Am., Spec. Pap. 215, 127–138, 1987.

77 R.S. Cohen and R.K. O'Nions, Identification of recycled continental material in the mantle from Sr, Nd and Pb isotope investigations, Earth Planet. Sci. Lett. 61, 73–84, 1982.

78 C.J. Hawkesworth, M.J. Norry, J.C. Roddick and R. Vollmer, $^{143}Nd/^{144}Nd$ and $^{87}Sr/^{86}Sr$ ratios from the Azores and their significance in LIL-element enriched mantle, Nature 280, 28–31, 1979.

79 W.M. White, B. Dupré and P. Vidal, Isotope and trace element geochemistry of sediments from the Barbados Ridge–Demerara Plain region, Atlantic Ocean, Geochim. Cosmochim. Acta 49, 1875–1886, 1985.

80 S.H. Richardson, J.J. Gurney, A.J. Erlank and J.W. Harris, Origin of diamonds in old enriched mantle, Nature 310, 198–202, 1984.

81 D. McKenzie and R.K. O'Nions, Mantle reservoirs and ocean island basalts, Nature 301, 229–231, 1983.

82 B.H. Hager, Subducted slabs and the geoid: constraints on mantle rheology and flow, J. Geophys. Res. 89, 6003–6015, 1984.

83 A.M. Dziewonski, Mapping the lower mantle: determination of lateral heterogeneity in P velocity up to degree and order 6, J. Geophys. Res. 89, 5929–5952, 1984.

84 K.C. Creager and T.H. Jordan, Aspherical structure of the

core-mantle boundary from PKP travel times, Geophys. Res. Lett. 13, 1497–1500, 1986.

85 J.L. Le Mouel, C. Gire and T. Madden, Motions at core surface in the geostrophic approximation, Phys. Earth Planet. Inter. 39, 270–287, 1985.

86 M. Stefanick and D.J. Jurdy, The distribution of hot spots, J. Geophys. Res. 89 (B12), 9919–9925, 1984.

87 M.F. Roden, Geochemistry of the earths's mantle, Nunivak Island, Alaska and other areas: evidence from xenolith studies, Ph.D. Dissertation, Massachusetts Institute of Technology, 1982 (unpublished).

88 C.J. Hawkesworth, N.W. Rogers, P.W.C. van Calsteren and M.A. Menzies, Mantle enrichment processes, Nature 311, 331–335, 1984.

89 W. Todt, R.A. Cliff, A. Hanser and A.W. Hofmann, $^{202}Pb + ^{205}Pb$ double spike for lead isotopic analyses, Terra Cognita 4, 209, 1984.

90 B. Barreiro, Lead isotopic compositions of South Sandwich island volcanic rocks and their bearing on magmagenesis in intra-oceanic island arcs, Geochim. Cosmochim. Acta 47, 817–822, 1983.

91 S.E. Church, The Cascade Mountains revisited: a re-evaluation in light of new lead isotopic data, Earth Planet. Sci. Lett. 29, 175–188, 1976.

92 P.H. Reynolds and E.J. Dasch, Lead isotopes in marine manganese nodules and the ore-lead growth curve, J. Geophys. Res. 76, 5124–5129, 1971.

93 P.L. Vidal and N. Clauer, Pb and Sr isotopic systematics of some basalts and sulfides from the East Pacific Rise at 21° N (project RITA), Earth Planet. Sci. Lett. 55, 237–246, 1981.

94 V.J.M. Salters, S.R. Hart and G. Panto, Origin of late Cenozoic volcanic rocks of the Carpathian Arc, Hungary, in: Pannonian Basin: A Study in Basin Evolution, L. Royden and F. Horvath, eds., AAPG/Hungarian Geological Society, Am. Assoc. Pet. Geol. Mem. 45, 279–292, 1988.

95 J.D. Kramers, J.C.M. Roddick and J.B. Dawson, Trace element and isotope studies on veined, metasomatic and "MARID" xenoliths from Bultfontein, South Africa, Earth Planet. Sci. Lett. 65, 90–106, 1983.

96 R.S. Cohen, R.K. O'Nions and J.B. Dawson, Isotope geochemistry of xenoliths from East Africa: implications for development of mantle reservoirs and their interaction, Earth Planet. Sci. Lett. 68, 209–220, 1984.

97 C. Alibert, A. Michard and F. Albarède, Isotope and trace element geochemistry of Colorado Plateau volcanics, Geochim. Cosmochim. Acta 50, 2735–2750, 1986.

98 C.J. Allègre, B. Dupré, B. Lambret and P. Richard, The subcontinental versus suboceanic debate, I. Lead-neodymium-strontium isotopes in primary alkali basalts from a shield area: the Ahaggar volcanic suite, Earth Planet. Sci. Lett. 52, 85–92, 1981.

99 G. Wörner, A. Zindler, H. Staudigel and H.-U. Schmincke, Sr, Nd, and Pb isotope geochemistry of Tertiary and Quaternary alkaline volcanics from West Germany, Earth Planet. Sci. Lett. 79, 107–119, 1986.

100 S.R. Hart and A. Zindler, In search of a bulk-Earth composition, Chem. Geol. 57, 247–267, 1986.

101 M.F. Roden, F.A. Frey and D.A. Clague, Geochemistry of tholeiitic and alkalic lavas from the Koolau Range, Oahu, Hawaii: implications for Hawaiian volcanism, Earth Planet. Sci. Lett. 69, 141–158, 1984.

102 P. Richard, N. Shimizu and C.J. Allègre, $^{143}Nd/^{146}Nd$ a natural tracer: an application to oceanic basalt, Earth Planet. Sci. Lett. 31, 269–278, 1976.

103 C.J. Allègre and M. Condomines, Basalt genesis and mantle structure studied through Th-isotopic geochemistry, Nature 299, 21–24, 1982.

104 B. Dupré and C.J. Allègre, Pb-Sr-Nd isotopic correlation and the chemistry of the North Atlantic mantle, Nature 286, 17–22, 1980.

105 R.S. Cohen, N.M. Evensen, P.J. Hamilton and R.K. O'Nions, U-Pb, Sm-Nd and Rb-Sr systematics of mid-ocean ridge basalt glasses, Nature 283, 149–153, 1980.

106 C.J. Allègre, Th. Staudacher and Ph. Sarda, Rare gas systematics: formation of the atmosphere, evolution and structure of the Earth's mantle, Earth Planet. Sci. Lett. 81, 127–150, 1986/87.